

A Novel GLP1 Receptor Interacting Protein ATP6ap2 Regulates Insulin Secretion in Pancreatic Beta Cells*

Received for publication, March 3, 2015, and in revised form, July 27, 2015. Published, JBC Papers in Press, August 13, 2015, DOI 10.1074/jbc.M115.648592

Feihan F. Dai, Alpana Bhattacharjee, Ying Liu, Battsetseg Batchuluun, Ming Zhang, Xinye Serena Wang, Xinyi Huang, Lemieux Luu, Dan Zhu, Herbert Gaisano, and Michael B. Wheeler¹

From the Departments of Physiology and Medicine, University of Toronto, Toronto, Ontario M5S 1A8, Canada

Background: The transduction of the GLP1 receptor (GLP1R) requires interactions with accessory proteins.

Results: ATP6ap2, also known as the renin receptor, was shown to interact with GLP1R and to regulate both GLP1 and glucose-stimulated insulin secretion.

Conclusion: ATP6ap2 is a novel GLP1R interactor that modulates insulin secretion.

Significance: Our study provides new insights into the fine-tuning GLP1R signaling in beta cells.

GLP1 activates its receptor, GLP1R, to enhance insulin secretion. The activation and transduction of GLP1R requires complex interactions with a host of accessory proteins, most of which remain largely unknown. In this study, we used membrane-based split ubiquitin yeast two-hybrid assays to identify novel GLP1R interactors in both mouse and human islets. Among these, ATP6ap2 (ATPase H⁺-transporting lysosomal accessory protein 2) was identified in both mouse and human islet screens. ATP6ap2 was shown to be abundant in islets including both alpha and beta cells. When GLP1R and ATP6ap2 were co-expressed in beta cells, GLP1R was shown to directly interact with ATP6ap2, as assessed by co-immunoprecipitation. In INS-1 cells, overexpression of ATP6ap2 did not affect insulin secretion; however, siRNA knockdown decreased both glucose-stimulated and GLP1-induced insulin secretion. Decreases in GLP1-induced insulin secretion were accompanied by attenuated GLP1 stimulated cAMP accumulation. Because ATP6ap2 is a subunit required for V-ATPase assembly of insulin granules, it has been reported to be involved in granule acidification. In accordance with this, we observed impaired insulin granule acidification upon ATP6ap2 knockdown but paradoxically increased proinsulin secretion. Importantly, as a GLP1R interactor, ATP6ap2 was required for GLP1-induced Ca²⁺ influx, in part explaining decreased insulin secretion in ATP6ap2 knockdown cells. Taken together, our findings identify a group of proteins that interact with the GLP1R. We further show that one interactor, ATP6ap2, plays a novel dual role in beta cells, modulating both GLP1R signaling and insulin processing to affect insulin secretion.

GLP1² is an incretin hormone secreted from enteroendocrine L cells in the intestines. The ability of GLP1 to enhance

insulin secretion upon stimulation by the uptake of glucose has been well documented (1–5). Furthermore, GLP1 has been shown to increase beta cell proliferation possibly through the TCF7L2/Wnt pathway (6–8). In addition to its effects in pancreatic beta cells, GLP1 also has diverse functions in a variety of extrapancreatic tissues. In the heart, the cardiac effects of GLP1 analogs have led to the amelioration of myocardial ischemia and to the restriction of infarct size (9), and GLP1 infusion could improve heart function (10). GLP1 in plasma was associated with blood pressure levels in a human population study (11). Further, GLP1 or its analogs were shown to lower blood pressure in rodents and human subjects (12–14). In the brain, GLP1 analogs induced the proliferation of neuronal progenitor cells, implicating a potential involvement in the repair of neurons (15–17).

The physiological and pharmacological effects of GLP1 are mediated by the GLP1 receptor (GLP1R), a member of the B class G protein-coupled receptor (GPCR) family (18). GLP1R is widely expressed in pancreatic islets, as well as in the brain, heart, kidney, and gastrointestinal tract (19–21). Specifically in the pancreas, GLP1R expression was confirmed in beta and delta cells; however, it was 10-fold lower in delta cells when quantified by quantitative real time PCR (qPCR) (21). In the alpha cell population, very low expression of GLP1R was detected (21). Like other B class GPCRs, GLP1R signals through the G_s protein complex and activates adenylyl cyclase, which converts ATP into cAMP (22, 23). The increased intracellular accumulation of cAMP triggers both the PKA and Epac2 pathways that are the common downstream pathways responsible for a number of GLP1-induced intracellular actions (24–26). In addition to classical PKA and Epac2 signaling, GLP1R is also found to activate PI3K signaling by transactivating the EGF receptor (27, 28).

As is the case with many GPCRs, a wide number of receptor activities and modes of signal transduction have been described for the GLP1R. This phenomenon may be explained in part by an interaction of the receptor with a large number of G protein-

* This work was supported by a grant from a Novo Nordisk Innovation Award and Canadian Institutes of Health Research MOP-102588 (to M. B. W.), Banting and Best Diabetes Center (BBDC) postdoctoral fellowships (to Y. L. and M. Z.), a BBDC graduate student award (to X. H.), and a BBDC summer student award (to X. W.). The authors declare that they have no conflicts of interest with the contents of this article.

¹ To whom correspondence should be addressed: Dept. of Physiology, 1 King's College Cir., Rm. 3352, Toronto, ON M5S 1A8, Canada. Tel.: 416-978-6737; Fax: 416-978-4940; E-mail: michael.wheeler@utoronto.ca.

² The abbreviations used are: GLP1, glucagon-like peptide 1; GLP1R, GLP1 receptor; ATP6ap2, ATPase H⁺-transporting lysosomal accessory protein

2; MYTH, membrane-based split ubiquitin yeast two-hybrid; GPCR, G protein-coupled receptor; qPCR, quantitative real time PCR; TF, transcription factor; GSIS, glucose-stimulated insulin secretion.

ATP6ap2 Regulates Insulin Secretion

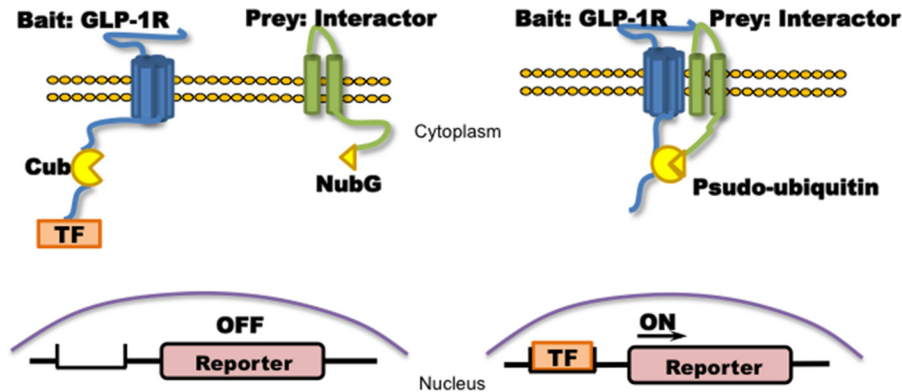


FIGURE 1. **Membrane-based split ubiquitin yeast two-hybrid.** *Left panel*, membrane-bound ubiquitin protein was split into two halves: C terminus (Cub) and N terminus (Nub, NubG is point mutation of Nub to avoid self-activation). Cub is associated with a TF that was fused to the bait GLP1R as GLP1R-Cub, and NubG was fused to the prey interactors as interactor-NubG. *Right panel*, if the bait interacts with the prey, the resulting proximity of the ubiquitin halves induced by the interaction will enable the reconstitution of Cub and NubG to form a functional pseudoubiquitin protein. Reconstitution recruits ubiquitin-specific proteases that cleave TF downstream of Cub, allowing the TF to translocate into the nucleus to initiate the transcription of reporter genes, which serve as readout of MYTH. As a result, the MYTH system does not rely on protein expression within the nucleus as does the traditional yeast two-hybrid system and can be used to study membrane-bound proteins such as GLP1R and its interactors.

dependent and independent accessory proteins (interactors). Receptor accessory proteins are reported to regulate GPCRs to target subcellular trafficking and intracellular signaling (29). For instance, KCTD isoforms 8, 12, 12b, and 16 are accessory proteins of the GABAB receptor and are indispensable for its function. These isoforms associate tightly with the GABAB2 receptor C terminus to increase agonist potency and markedly alter G protein signaling, thus accelerating the onset of signaling and promoting desensitization of the receptor in a subtype-specific manner (30). However, very little is known thus far on GLP1R accessory proteins. It has been reported that the GLP1R interactor scaffolding protein β -arrestin-1, a protein involved in GPCR agonist-induced desensitization and endocytosis, is required to stimulate cAMP production and insulin secretion in INS-1 beta cell lines upon physical association with the GLP1R (31). Furthermore, the GLP1 interactor caveolin-1 directly interacts with GLP1R, which may in part be directing the trafficking of GLP1R to lipid rafts (32). In another study, β -arrestin-1 was shown to associate with GLP1R and c-Src as a complex, which is required for the proliferative action of GLP1 (33). According to our model, these reports raise the possibility that GLP1R could be coupled to many accessory/interacting proteins to form multimeric protein interactome complexes capable of transducing context-specific downstream signaling pathways that lead to an increasing number of cellular actions.

Recently, using a novel membrane-based split-ubiquitin yeast two-hybrid system (MYTH), we discovered a series of GLP1R interacting proteins in human fetal brain that were shown to attenuate GLP1R activity (34). In this current study, we used MYTH to reveal a GLP1R interactome in both mouse and human islets: two tissues where GLP1R agonists have profound and clinically relevant effects. This MYTH screen identified a host of novel putative GLP1R interacting proteins with major differences seen between human and mouse islet libraries. However, one interactor, ATP6ap2 (ATPase H⁺-transporting lysosomal accessory protein 2), identified in both mouse and human islet screens was shown to be abundantly expressed in pancreatic islets. Further work demonstrated that ATP6ap2

regulated insulin secretion from pancreatic beta cells in both glucose and GLP1R dependent modalities.

Experimental Procedures

Cell Culture—MIN6 cells (a gift from Dr. Susumu Seino from Kobe University, Kobe, Japan) were maintained in DMEM (Life Technologies Inc.) containing 10% FBS, 100 units/ml penicillin G sodium, and 100 μ g/ml streptomycin sulfate at 37 °C in 5% CO₂. INS-1 832/3 cells (from Dr. Chris Newgard, Duke University, Durham, NC) were maintained in RPMI 1640 (11.1 mM D-glucose) supplemented with 10% FBS, 100 units/ml penicillin, 100 μ g/ml streptomycin, 10 mM HEPES, 2 mM L-glutamine, 1 mM sodium pyruvate, and 50 μ M mercaptoethanol. Human GLP1R overexpressing CHO cells (RC2) were maintained in DMEM containing 10% FBS, 100 units/ml penicillin G sodium, and 100 μ g/ml streptomycin sulfate at 37 °C in 5% CO₂. cDNA plasmids and siRNA were transfected into cells using Lipofectamine 2000 and Lipofectamine RNAiMAX (Invitrogen) according to the manufacturer's instructions. After transfection for 48 h, cells were used for analysis.

Isolation and Disperse of Mouse Islet—Mouse islets were isolated and dispersed from male CD-1 mice (~2 months of age) as described previously (35, 36). The intact islets were cultured in RPMI 1640 medium containing 11.1 mM glucose supplemented with 10% fetal bovine serum, 10 mM HEPES, 1% L-glutamate, 100 units/ml penicillin, and 100 μ g/ml streptomycin at 37 °C in 5% CO₂.

The Split Ubiquitin Membrane Yeast Two-hybrid System—The MYTH system (Fig. 1) methodology was described in detail in previous studies (34, 37). Briefly, MYTH is based on the "split ubiquitin system" (38–41) in which ubiquitin can be split into N-terminal (Nub) and C-terminal (Cub) halves. The reconstitution of the two halves forms pseudoubiquitin, which is recognized by ubiquitin specific proteases leading to proteasomal degradation. In the MYTH system, the receptor (in this case GLP1R) is fused with Cub followed by a transcription factor (TF) to form the "bait," whereas the interactor protein is fused with NubG (mutational Nub Ile¹³ → Gly to reduce the affinity

TABLE 1
Sequence of primers

Name	Access number	Species	Primer sequences	
			Forward	Reverse
Atp6ap2	NM_027439	Mouse	5'-GTTTTGCAAGTGGCTCCCAG-3'	5'-GCCGCAATGTGACTGAAAGG-3'
Aig1	NM_025446	Mouse	5'-TTCTTCGGCATCTGTGTGCT-3'	5'-CTGTCTTCTTGTCTCCTGGT-3'
Aph1b	NM_177583	Mouse	5'-TCATGGGCATCTGGGCATTT-3'	5'-TCCTTGTCTTGGCAGAGCAG-3'
Gnas	NM_001077507	Mouse	5'-CAGCCTGAAGCAATGGATGC-3'	5'-CGTAGGAGCTCCAGCATCAG-3'
Gpr108	NM_030084	Mouse	5'-TCGTGCTCACTGGCTACAAG-3'	5'-TCCTCCTCATCCTCCTGTGG-3'
Iftm3	NM_025378	Mouse	5'-GGATCGGAAGATGGTGGTG-3'	5'-CCATCAGGATGCTGAGGACC-3'
ZIP13	NM_026721	Mouse	5'-TGACTGTAACAGGGTCCCCA-3'	5'-CTGCCTGTGCGCTGGATAAT-3'
ZIP7	NM_008202	Mouse	5'-GACAGTGTCCAGGTGGTGT-3'	5'-CATGGCCACTCCCACGATAG-3'
Ly6e	NM_001164040	Mouse	5'-TGTCAACCTTGGCTACACCC-3'	5'-CGCCACACCGAGATTTGAGAT-3'
Syngn4	NM_021482	Mouse	5'-CTCTCCATCATCCACCAGCC-3'	5'-AGTCGTATGTAGGGGGACA-3'
Selk	NM_019979	Mouse	5'-CCAGGAAACCCCTCCACGAAG-3'	5'-TCATCCACCAGCCATTGGAG-3'
Vamp3	NM_009498	Mouse	5'-TGCCTCGCAGTTTGGAAACAAG-3'	5'-GAGAGTCAGCCCGTGGATAC-3'
Slc2a5	NM_019741	Mouse	5'-CGAAAACCTACGAGGGGCT-3'	5'-GAGACTCCGAAGGCCAAACA-3'
Leprotl1	NM_026609	Mouse	5'-ATGAGCAACCGGTGTAAGGA-3'	5'-GCTCTGGCAAACAACAGG-3'
Kcnj11	NM_010602	Mouse	5'-TGATCCCCATGGAGAATGG-3'	5'-TCGATGAGCGGTAGATGATGAG-3'
β -Actin	NM_007393.3	Mouse	5'-CTGAATGGCCAGGTCTGA-3'	5'-CCCTGGCTGCCTCAACAC-3'
Zip7	NM_001008885	Rat	5'-CGGCGCTTTCATGCTTTTA-3'	5'-GCTCTAGCCTTTGATCCGCA-3'
Zip13	NM_001039196	Rat	5'-CCACTGTCACTAGCAGCAA-3'	5'-TGGGCTGGTTTCTTTGTC-3'
Leprotl1	NM_001013188	Rat	5'-GAGCAACGCTTGTAAAGGAGC-3'	5'-TGGCAAACACTACAGGGAGC-3'
Selk	NM_207589	Rat	5'-CGGTCTTCTCTGTGCTAGG-3'	5'-CCGGCTGTCTAACACCTGAC-3'
Gpr108	NM_199399	Rat	5'-CGCAGTGTGATGGGAATACT-3'	5'-GAGAGTCAGCCCGTGGATAC-3'
Syngn4	NM_001025644	Rat	5'-AGCTGGTCTCTGTCTTTC-3'	5'-TCTTAAAGCGGGTGCCTACC-3'
Iftm3	NM_001136124	Rat	5'-CTGATCTGACGTGCTCCAC-3'	5'-AGTGTACACCTGCGTGTTCG-3'
Aph1b	NM_001047090	Rat	5'-TGTCCCGCTTCTCTCTAA-3'	5'-GTGATGAGCGGTGATGATGAT-3'
Ly6e	NM_001017467	Rat	5'-TGTCAACCTTGGCTACACCC-3'	5'-TAGCTATTACGAGACGCCAC-3'
Slc2a5	NM_031741	Rat	5'-GACACCTACTACGACAGAAACA-3'	5'-CCAAGAATCCAACCATGAGAGA-3'
Gnas	NM_021845	Rat	5'-AACTGCCTCCACGGCAATAA-3'	5'-CCCTTGGGCTTCAAAGGTT-3'
Atp6ap2	NM_001007091	Rat	5'-TGCTGTGGCAACCTATTTC-3'	5'-CTGCATTCTCAAAGGTAAGA-3'
Aig1	NM_001134425	Rat	5'-GGCTGTATTCTTCGGCATCT-3'	5'-TTCCTGAGGTGTGCTTCTTG-3'
Vamp3	NM_009498	Rat	5'-AACTTGGTGTGCTGTCTCCTC-3'	5'-CGGGAACATTCACAGCTAAA-3'
PC1/3	NM_017091	Rat	5'-AGAGGCTCTGTGGTTCGAA-3'	5'-ACAAGGCACAAAGGGGAAA-3'
PC2	NM_012746.1	Rat	5'-TGGCGAGACATGCAACATCT-3'	5'-AATTCAGGCCAACCCATT-3'
CPE	NM_013128.1	Rat	5'-TGTGTGGCCTGGAAACTAT-3'	5'-AACAGCAGGCTGAAAGTAA-3'
KCNJ11	NM_031358	Rat	5'-AGTGTGGCTGTGGCAAAGG-3'	5'-GGACCCTCACTCAGGACAA-3'
β -Actin	NM_031144	Rat	5'-TAGCCATCCAGCTGTGTTG-3'	5'-GGAGCGCTAACCTCATAG-3'

TABLE 2
cDNA libraries of mouse and human islets

	Human islet library	Mouse islet library
Islet source	Nondiabetic human	CD1 mouse
Library prey vector	pPR3-N	pPR3-N
Cloning site	Directional/Sfi I	Directional/Sfi I
First strand synthesis	Oligo(dT)	Oligo(dT)
Complexity	5.6×10^6 independent clones	6.9×10^6 independent clones
Average insert size	1.04 kb	1.26 kb
Size range	0.5–5 kb	0.5–5 kb
Vectors with insert	100%	100%
Inserts > 250 bp	100%	100%

of Nub for Cub and avoid self-activation) to form the “prey.” When NubG interactors (prey) are transformed into yeast expressing GSRs-Cub-TF (bait), the interaction between bait and prey brings NubG and Cub to proximity with one another to form a functional pseudoubiquitin, resulting in the release of the TF upon recognition and cleavage of the pseudoubiquitin by ubiquitin specific proteases. The TF further translocates into the nucleus and induces the expression of reporter genes that serves as a readout of protein-protein interaction.

Construction of Human and Mouse Islet cDNA Libraries Compatible with MYTH—Mouse islets were isolated from CD-1 mice (~2 months of age) as described previously (35, 36, 42). Human islets from review board-approved healthy donors were provided by the Clinical Islet Laboratory (University of Alberta, Edmonton, Canada). The total RNA of human and mouse islets was prepared using the RNeasy mini kit (Qiagen) and were used to produce a cDNA library that was compatible to the MYTH system by Dualsystems Biotech, Inc. (Schlieren,

Switzerland). pPR3-N (Dualsystems Biotech, Inc.) was used as the prey vector for generating the cDNA library.

MYTH Analysis of GLP1R in Human and Mouse Islet cDNA Library—The MYTH analysis was performed by Dualsystems Biotech Inc. The technology and the bait vector pCCW-stehGLP1R-cub were described in previous studies (34, 37). Briefly, the bait and prey vector were co-transformed into *Saccharomyces cerevisiae* host THY.AP4 strain, and colony selection was performed on yeast minimal media/synthetic defined agar plates deficient of tryptophan, leucine, histidine, and adenine negative (–Trp/–Leu/–His/–Ade). All positively selected colonies were inoculated in yeast, and the plasmids harboring the interactor sequence were purified. The purified plasmids were amplified in *Escherichia coli* strain XL-10 Gold. All the plasmids were validated by sequencing. The candidates were compared against pre-existing MYTH screening databases from Dualsystem Biotech Inc., and only unique candidates identified in our current screen were chosen as putative interactors of GLP1R for further study.

cDNA Plasmids, siRNA, and qPCR—The cDNA plasmid pcDNA-ATP6ap2 was purchased from Origene (Rockville, MD) and the Midi-Prep Kit (Qiagen) was used for plasmid purification. Short interfering RNA (SMARTpool siRNA) or scrambled siRNA (control) were purchased from Dharmacon, Thermo Scientific (Waltham, MA). Total RNA from cells was prepared using the RNeasy mini kit (Qiagen) according to the manufacturer's instructions. Purified RNA was converted to cDNA using a Moloney murine leukemia virus reverse transcriptase cDNA kit (Sigma), and real time PCR was performed

TABLE 3
GLP1R interactors identified from human islet cDNA library by MYTH

Uniprot ID	Protein	Gene	Biological process	Molecular function	Subcellular localization
P55061	Bax inhibitor 1	TMBIM6	Suppressor of apoptosis; modulates unfolded protein response signaling; modulates endoplasmic reticulum calcium homeostasis by acting as a calcium leak channel	Calcium binding	Membrane
Q8N3C7	CAP-Gly domain-containing linker protein 4	CLIP4	No information	No information	No information
P08861	Chymotrypsin-like elastase family member 3B	CELA3B	Cholesterol metabolic process, proteolysis	Serine-type endopeptidase activity	No information
O95471	Claudin-7	CLDN7	Calcium-independent cell-cell adhesion	Identical protein binding, structural molecule activity	Integral component of membrane
Q9P0B6	Coiled-coil domain-containing protein 167	CCDC167	No information	No information	Membrane
P04118	Colipase	CLPS	Lipid catabolic process, small molecule metabolic process	Enzyme activator activity	Secreted, extracellular region
P61803	Dolichyl-diphosphooligosaccharide protein glycosyltransferase subunit DAD1	DAD1	Apoptosis	Dolichyl-diphosphooligosaccharide protein	Membrane
P63092	Guanine nucleotide-binding protein G _s subunit alpha isoforms short	GNAS	Activation of adenylate cyclase activity, GTPase activity	Signal transducer	Cell membrane
Q01628	Interferon-induced transmembrane protein 3	IFITM3	Immunity, IFN-induced antiviral protein which disrupts intracellular cholesterol homeostasis	Antiviral protein	Cell membrane
O75556	Mammaglobin-B	SCGB2A1	Androgen binding, transcriptional regulation of steroid hormones	Steroid binding	Extracellular region
Q9Y6C9	Mitochondrial carrier homolog 2	MTCH2	Transport, induces mitochondrial depolarization	Transporter	Mitochondrion inner membrane
P55259	Pancreatic secretory granule membrane major glycoprotein GP2	GP2	Antigen transcytosis by M cells in mucosal-associated lymphoid tissue	Antigen binding	Cell membrane, secreted
P19021	Peptidyl-glycine α -amidating monooxygenase	PAM	Peptidylamidoglycolate lyase activity, peptidylglycine monooxygenase activity, protein binding, peptide metabolic process, protein modification process	Ion/protein binding	Membrane
Q9NPR9	Protein GPR108	GPR108	No information	No information	Membrane
Q8N2A0	Putative uncharacterized protein encoded by LINC00269	LINC00269	No information	No information	No information
Q9NQC3	Reticulon-4	RTN4	Neurogenesis, developmental neurite growth regulatory factor with a role as a negative regulator of axon-axon adhesion and growth, and as a facilitator of neurite branching	Regulatory factor	Endoplasmic reticulum membrane
Q9BY50	Signal peptidase complex catalytic subunit SEC11C	SEC11C	Serine-type peptidase activity, proteolysis, regulation of insulin secretion, signal peptide processing, SRP-dependent cotranslational protein targeting to membrane	Serine-type peptidase activity	Integral component of membrane
O95473	Synaptogyrin-4	SYNGR4	No information	No information	Membrane
P48230	Transmembrane 4 L6 family member 4	TM4SF4	No information	No information	Integral component of membrane
Q6UWJ1	Transmembrane and coiled-coil domain-containing protein 3	TMCO3	Hydrogen ion transmembrane transport; probable Na ⁺ /H ⁺ antiporter	Solute:hydrogen antiporter activity	Membrane
P07478	Trypsin-2	PRSS2	Calcium ion binding, protein binding, serine-type endopeptidase activity, regulation of cell adhesion, regulation of cell growth, proteolysis	Calcium binding	Secreted, extracellular region
Q8WVX3	Uncharacterized protein C4orf3	C4orf3	No information	No information	Membrane
Q9NVV5	Androgen-induced gene 1 protein	AIG1	No information	No information	Membrane
P0C6T2	Dolichyl-diphosphooligosaccharide protein glycosyltransferase subunit 4	OST4	Involved in N-glycosylation	Component of the oligosaccharyltransferase complex	Membrane
P54851	Epithelial membrane protein 2	EMP2	Cell proliferation, adhesion	Regulatory factor	Membrane
P03901	NADH-ubiquinone oxidoreductase chain 4L	MT-ND4L	Mitochondrial electron transport, NADH to ubiquinone, small molecule metabolic process	NADH dehydrogenase (ubiquinone) activity	Integral component of membrane
Q9P003	Protein cornichon homolog 4	CNIH4	Intracellular signal transduction	Signal transducer	Membrane
O75787	Renin receptor	ATP6A2	Protein binding, receptor activity, angiotensin maturation, positive regulation of transforming growth factor β 1 production, regulation of MAPK cascade	Aspartic-type endopeptidase activity, receptor activity	Membrane
O95197	Reticulon-3	RTN3	Apoptotic process, response to stress, vesicle-mediated transport	Protein binding	Endoplasmic reticulum membrane, Golgi apparatus membrane
Q9Y6D0	Selenoprotein K	SELK	Calcium, ion transport	Transporter	Integral component of membrane
Q96B49	Mitochondrial import receptor subunit TOM6 homolog	TOMM6	Protein transport, cellular protein metabolic process	Transporter	Mitochondrion outer membrane

TABLE 4
GLPIR interactors identified from mouse islet cDNA library by MYTH

Uniprot ID	Protein	Gene	Biological process	Molecular function	Subcellular localization
Q9CXR1	Dehydrogenase/reductase SDR family member 7	DHR57	Nucleotide binding, oxidoreductase	Oxidoreductase activity	No information
Q9D0P0	Emopamil-binding protein-like	EBPL	Cholesterol delta-isomerase activity, sterol metabolic process	Cholesterol delta-isomerase activity	Integral component of membrane
Q8C7N7	γ -Secretase subunit APH-1B	APH1B	Endopeptidase activity, Notch signaling pathway, positive regulation of catalytic activity, protein processing	Endopeptidase activity	Membrane
Q9Z186	Glucose-6-phosphatase 2	G6PC2	Glucose-6-phosphatase activity, gluconeogenesis, regulation of insulin secretion	Hydrolase activity	Integral component of membrane
Q64Z53	Lymphocyte antigen 6E	LY6E	Adrenal gland development, epinephrine secretion, in utero embryonic development, organ growth, ventricular cardiac muscle tissue morphogenesis	Antigen	Cell membrane
Q99N07	Membrane-spanning 4-domains subfamily A member 6D	MS4A6D	Involved in signal transduction as a component of a multimeric receptor complex.	Receptor	Cell membrane
Q9DCL9	Multifunctional protein ADF2	PAICS	Purine biosynthesis	Decarboxylase, ligase, lyase	No information
Q9Z2U0	Proteasome subunit α type-7	PSMA7	Ubiquitin-dependent protein catabolic process	Threonine-type endopeptidase activity	Cytoplasm, nucleus, proteasome
Q9DA39	Protein lifeguard 4	TMBIM4	Anti-apoptosis, apoptotic process, regulation of calcium-mediated signaling	Anti-apoptotic protein	Integral component of membrane
Q9Z2E9	Seipin	BSC12	Lipid metabolism and degradation, regulator of lipid catabolism essential for adipocyte differentiation	Regulator protein	Integral component of endoplasmic reticulum membrane
Q8R207	Serine palmitoyltransferase small subunit A	SPTSSA	Sphingolipid metabolism, lipid metabolism	Serine C-palmitoyltransferase activity	Integral component of membrane
Q9WV38	Solute carrier family 2, facilitated glucose transporter member 5	SLC2A5	Hexose transmembrane transport, cellular response to fructose stimulus	Glucose/fructose transmembrane transporter activity	Integral component of membrane
Q9Z2I6	Tetraspanin-2	TSPAN2	Brain development	Signal transduction	Integral component of membrane
P63024	Vesicle-associated membrane protein 3	VAMP3	SNARE involved in vesicular transport from the late endosomes to the <i>trans</i> -Golgi network	SNAP receptor activity, SNARE binding	Integral component of membrane
Q31125	Zinc transporter SLC39A7	SLC39A7	Zinc ion transport	Metal ion transmembrane transporter activity	Integral component of membrane
Q8BZH0	Zinc transporter ZIP13	SLC39A13	Zinc influx transporter, cellular zinc ion homeostasis	Zinc ion transmembrane transporter activity	Integral component of membrane
P27659	60 S ribosomal protein L3	RPL3	Translation, cellular response to interleukin-4	Structural constituent of ribosome	Nucleus, cytoplasm
P01887	β 2-Microglobulin	B2M	MHC class I protein complex, antigen processing and presentation of peptide antigen via MHC class I, immune response	Antigen presentation	Secreted, extracellular region
P00158	Cytochrome b	MTT-CYB	Component of the ubiquinol-cytochrome c reductase complex (complex III or cytochrome <i>b-c₁</i> complex), respiratory electron transport chain	Electron carrier activity, oxidoreductase activity	Mitochondrion inner membrane
Q9Z324	Dolichol phosphate-mannose biosynthesis regulatory protein	DPM2	Biosynthetic process of dolichol phosphate-mannose	Dolichyl-phosphate β -D-mannosyltransferase activity	Endoplasmic reticulum membrane
Q9CQE7	Endoplasmic reticulum-Golgi intermediate compartment protein 3	ERGIC3	Endoplasmic reticulum to Golgi vesicle-mediated transport	Transport protein	Endoplasmic reticulum membrane, Golgi apparatus
Q9CQ74	Leptin receptor overlapping transcript-like 1	LEPROTL1	Regulates growth hormone receptor cell surface expression in liver	Regulator protein	Membrane
Q60961	Lysosomal-associated transmembrane protein 4A	LAPTM4A	Transport of nucleosides and/or nucleoside derivatives between the cytosol and the lumen of an intracellular membrane-bound compartment	Transport protein	Endomembrane system, plasma membrane
P03925	NADH-ubiquinone oxidoreductase chain 6	MTND6	Core subunit of the mitochondrial membrane respiratory chain NADH dehydrogenase (complex I)	NADH dehydrogenase (ubiquinone) activity	Integral component of membrane, mitochondria membrane
Q9CQS8	Protein transport protein Sec61 subunit β	SEC61B	Protein translocation, transport	Ribosome binding	Endoplasmic reticulum and membrane
Q9CYN9	Renin receptor	ATP6AP2	Protein binding, receptor activity, angiotensin maturation, positive regulation of transforming growth factor β 1 production, regulation of MAPK cascade	Aspartic-type endopeptidase activity, receptor activity	Membrane
Q9JLJ1	Selenoprotein K	SELK	Calcium, ion transport	Transporter	Integral component of membrane
P97858	Solute carrier family 35 member B1	SLC35B1	Carbohydrate transport	Transport protein	Endoplasmic reticulum membrane
Q9CQ56	Vesicle transport protein USE1	USE1	Endoplasmic reticulum tubular network organization, regulation of endoplasmic reticulum to Golgi vesicle-mediated transport	Transporter	Endoplasmic reticulum membrane

ATP6ap2 Regulates Insulin Secretion

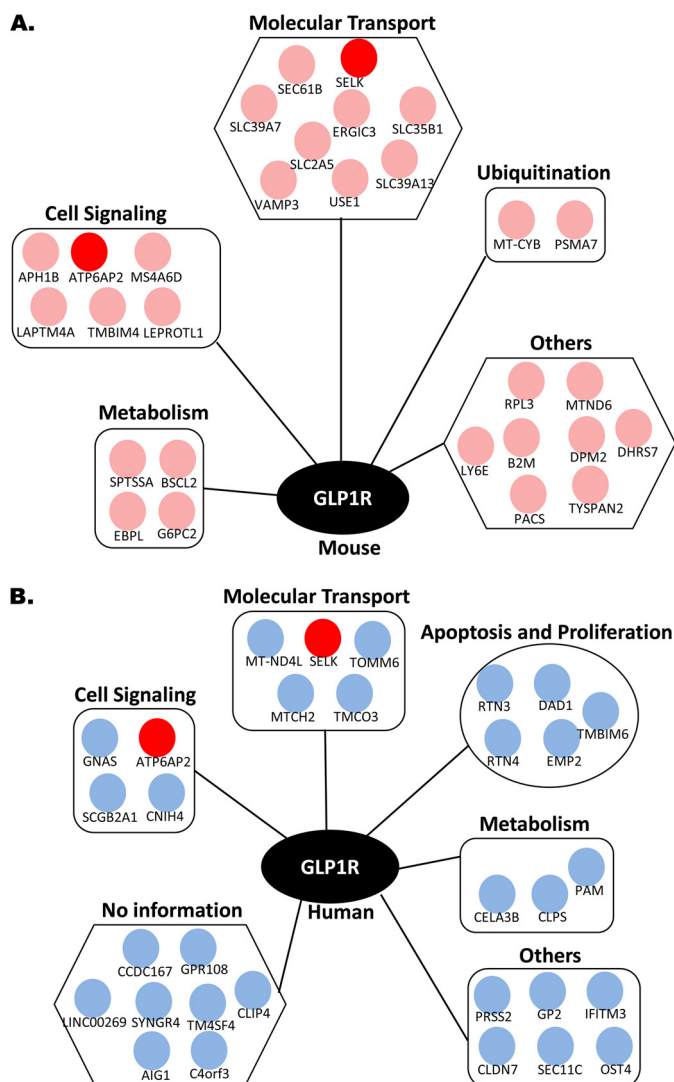


FIGURE 2. Interactor networks of GLP1R identified from human and mouse islet MYTH screens. A and B, mouse islet (A) and human islet (B) cDNA libraries. Each interactor is represented by a separate dot. Pink dots represent interactors identified in mouse islets, and blue dots represent interactors identified in human islets. Interactors common to both mouse and human islets are identified in red.

using an ViiA7 real time PCR system (Applied Biosystems, Foster City, CA) according to the same protocol described in previous studies (43). A standard curve was generated using mouse genomic DNA for quantification purposes. The measurements of gene expression were normalized to β -actin transcripts within the same sample. The sequences of the primers are shown in Table 1.

Co-immunoprecipitation and Immunoblotting—INS-1 cells co-transfected with GLP1R-His-V5-tagged and FLAG-tagged interactor were washed with ice-cold PBS containing 137 mM NaCl, 2.7 mM KCl, 10 mM Na_2HPO_4 , and 1.76 mM KH_2PO_4 to a pH of 7.4. Cells were harvested in lysis buffer containing 10% glycerol, 50 mM HEPES, 150 mM NaCl, 2 mM EDTA, 0.25% *n*-dodecyl- β -D-maltoside with complete protease inhibitor mixture (Hoffmann-La Roche Limited, Ltd., Mississauga, Canada). M2 Anti-FLAG affinity gel (Sigma-Aldrich) was used to pull down FLAG-tagged interactor proteins. Briefly, the cell extract (supernatant) was incubated with anti-FLAG-aga-

rose that was equilibrated with wash buffer (0.1% digitonin, 5 mM imidazole with protease inhibitor mixture) for 2 h at 4 °C. The anti-FLAG affinity beads were washed three times with wash buffer and eluted in 2 \times SDS loading buffer. The precipitated proteins from each sample were loaded and separated on a 10% polyacrylamide gel and transferred to PVDF-plusTM membrane for immunoblotting. Anti-V5 (Invitrogen, 1:2500 dilution), anti-FLAG primary antibodies (Sigma-Aldrich, 1:2000 dilution), and HRP-conjugated mouse secondary antibody were used, and the fluorescence signal was detected by Amersham Biosciences enhanced chemiluminescence (GE Healthcare Lifesciences) with images acquired by the Kodak Image Station 4000 Pro (Carestream Health Inc., Rochester, NY).

Immunohistochemistry—Tissues and cells were fixed in 10% neutral buffered formalin, dehydrated in 70% ethanol, and embedded in paraffin. Paraffinized samples were sliced (5 μm) and adhered to glass slides, rehydrated, and blocked with 3% H_2O_2 for 30 min. Following PBS washing, sections were incubated in nonimmune serum-free protein block solution (Dako Canada Inc., Burlington, Canada) for 30 min. Sections were blotted to remove excess blocking solution prior to overnight application of primary anti-ATP6ap2 antibody (Sigma-Aldrich, 1:500 dilution) and anti-insulin (Invitrogen, 1:100 dilution) at 4 °C. Images of each section were acquired using Aperio Imagescope version 11.0.2.725 (Aperio Technologies, Vista, CA).

Immunofluorescence and Confocal Microscopy—The expression of ATP6ap2 was determined in dispersed human islets from both normal and type 2 diabetic donors (44) with primary anti-ATP6ap2 (1:125, Sigma), and the cells were co-stained with anti-insulin (1:100, Dako) and anti-glucagon (1:2000, Sigma), followed by Alexa Fluor[®] 488 goat anti-mouse (1:500, Molecular Probes, Life Technologies), Alexa Fluor[®] 555 donkey anti-rabbit (1:500, Molecular Probes, Life Technologies), or Alexa Fluor[®] 488 donkey anti-guinea pig (1:500, Jackson ImmunoResearch, West Grove, PA) secondary antibody. Images were acquired on LSM510 Zeiss confocal microscope (Zeiss) at 40 \times magnification with an oil lens. The relative fluorescence intensity was quantified using LSM510 software and normalized by area.

Glucose-stimulated Insulin Secretion and Intracellular cAMP Assays—Glucose-stimulated insulin secretion (GSIS) studies were carried out as previously described (43). Briefly, cells were preincubated for 2 h in 2.5 mM glucose HEPES balanced salt solution (114 mM NaCl, 4.7 mM KCl, 1.2 mM KH_2PO_4 , 1.16 mM MgSO_4 , 2.5 mM CaCl_2 , 25.5 mM NaHCO_3 , 20 mM HEPES, and 0.2% (w/v) bovine serum albumin, essentially fatty-acid free, pH7.2) and then in the same HEPES balanced salt solution buffer containing different indicated glucose concentrations for 1 h with 30 nM GLP1 (GLP1-induced insulin secretion) (Bachem Inc., Torrance, CA). Insulin secreted was measured using the homogenous time-resolved fluorescence kit (Cisbio Bioassays, Bedford, MA) and normalized to total protein content. Intracellular cAMP content was measured as previously described (42, 34) by using the homogenous time-resolved fluorescence assay kit (Cisbio Bioassays). Cells were incubated for 1 h with cryptate anti-cAMP antibody

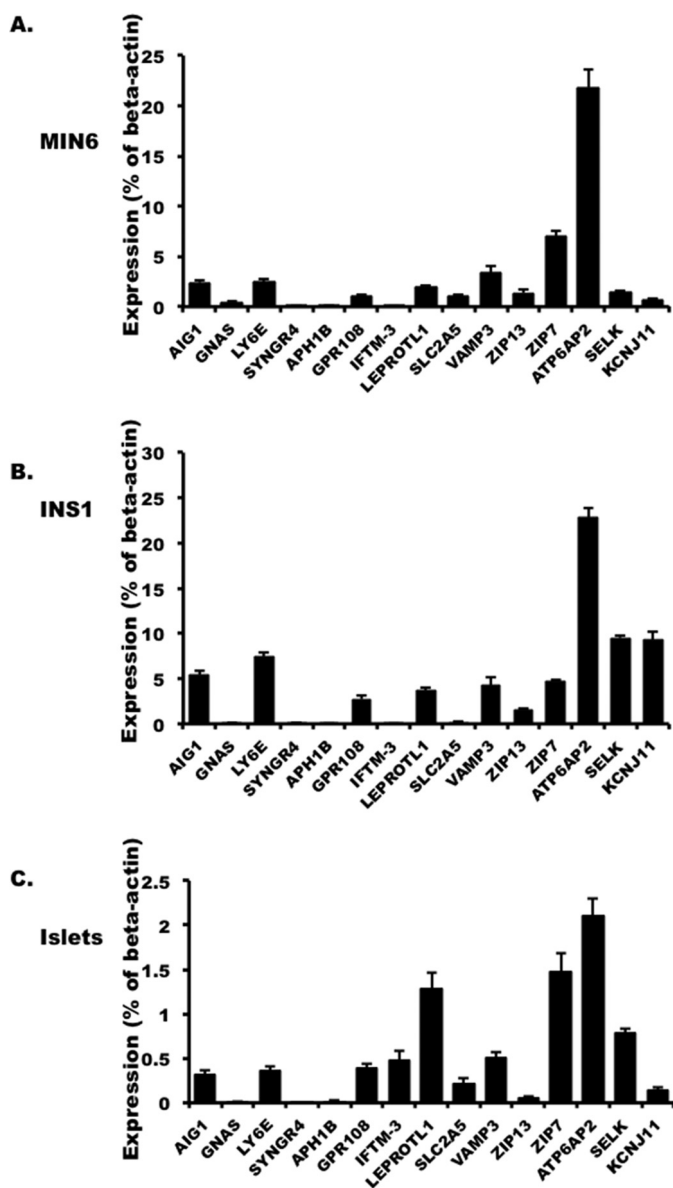


FIGURE 3. The expression of selected interactors in MIN6 (A), INS1 832/3 cells (B), and mouse islets (C) presented as the percentage of β -actin in the cell. The values are represented by the averages \pm S.E. from triplicates in three independent experiments.

and D2-labeled cAMP. Fluorescence signals in both insulin and cAMP assays were measured using the PHERAstar Plus microplate reader (BMG LABTECH, Guelph, Canada).

Transmission Electron Microscopy—Cells were fixed, and images were acquired as previously described (45). Briefly, the samples were observed under a Philips CM100 electron microscope operating at 75 kV. Images were recorded digitally using Kodak 1.6 Megapixels camera system operated using AMT software (Advanced Microscopy Techniques Corporation). Granule numbers were manually quantified using ImageJ software (45).

High Content Imaging—Images were acquired and analyzed on a Thermo Fisher Cellomics ArrayScan[®] VTI HCS reader using iDEV[™] software. The filter settings for each dye were excitation/emission: 577/590 nm for LysoTracker Red DND-99, excitation/emission: 494/516 nm for Fluo4AM, and excita-

tion/emission: 350/461 nm for Hoechst 33342 (Molecular Probes, Life Technologies). Each dye was loaded into live INS-1 cells or dispersed mouse islet cells according to the manufacturer's recommendation.

Statistics—Paired *t* tests were performed to determine statistical significance. *p* values less than 0.05 were considered statistically significant.

Results

Generation and Analysis of Human and Mouse Islet cDNA Libraries—To better understand the mechanisms through which GLP1R fine tunes the regulation of insulin secretion, we generated cDNA libraries from both human and mouse islets that were equipped with the physiological machinery necessary for insulin secretion. GLP1R was shown to be abundantly expressed in islet beta cells, less in delta cells, and very low in alpha cells (21). As such, we reasoned that isolated human and mouse islets would serve as reasonable models to study the GLP1R interactome in the setting of the pancreatic beta cell. Using purified RNA from isolated human and mouse islets, we generated human and mouse islet cDNA libraries with the complexity and titer required for MYTH screening. The human islet cDNA library generated contained $\sim 5.6 \times 10^6$ independent clones, ranging in sizes from 0.5 to 5.0 kb with 100% of all vectors containing cDNA inserts. The mouse islet library contained 6.9×10^6 independent clones with a size range equal to that of the human islet library generated (Table 2).

MYTH Analysis of GLP1R in Human and Mouse Islets (Functional Involvement)—The structure of the bait vector overexpressing human GLP1R and its ability to respond to GLP1 was previously described by Huang *et al.* (34). By using the bait GLP1R vector, we observed 43 positive interactor proteins from the human islet library and 37 such interactor proteins from the mouse islet library. By eliminating highly abundant proteins and common nonspecific MYTH screen interactors (those interactors that appeared in over 50% and 20–50% of all performed MYTH screens done by Dualsystems Biotech Inc.), we obtained 31 and 29 unique interacting proteins from the human (Table 3) and the mouse islet libraries (Table 4), respectively. Apart from $G\alpha_s$, which is known to be linked to GLP1R function, these putative interactors identified in the MYTH screen have not previously been described with GLP1R. Collectively they represent many known functional groups such as intracellular transport, metabolism and ion transport, or signal transduction (Fig. 2). Some interactors were suggested to be relevant to pancreatic beta cell function, such as zinc transporters (SLC39A7 and SLC39A13), fructose transporters (SLC2A5), and insulin exocytotic SNARE proteins (VAMP3) etc. Among the putative interactors, ATP6ap2 and SELK were identified as two proteins present in both the human and mouse islet library screens (Fig. 2).

Expression of Selected Interactors in Pancreatic Beta Cells—Because ATP6ap2 and SELK were identified from both libraries, we examined their expression using qPCR in three distinct sources of pancreatic beta cells (MIN6, INS1, and isolated mouse islets). Since the GLP1R is primarily expressed at the plasma membrane, we also included 11

ATP6ap2 Regulates Insulin Secretion

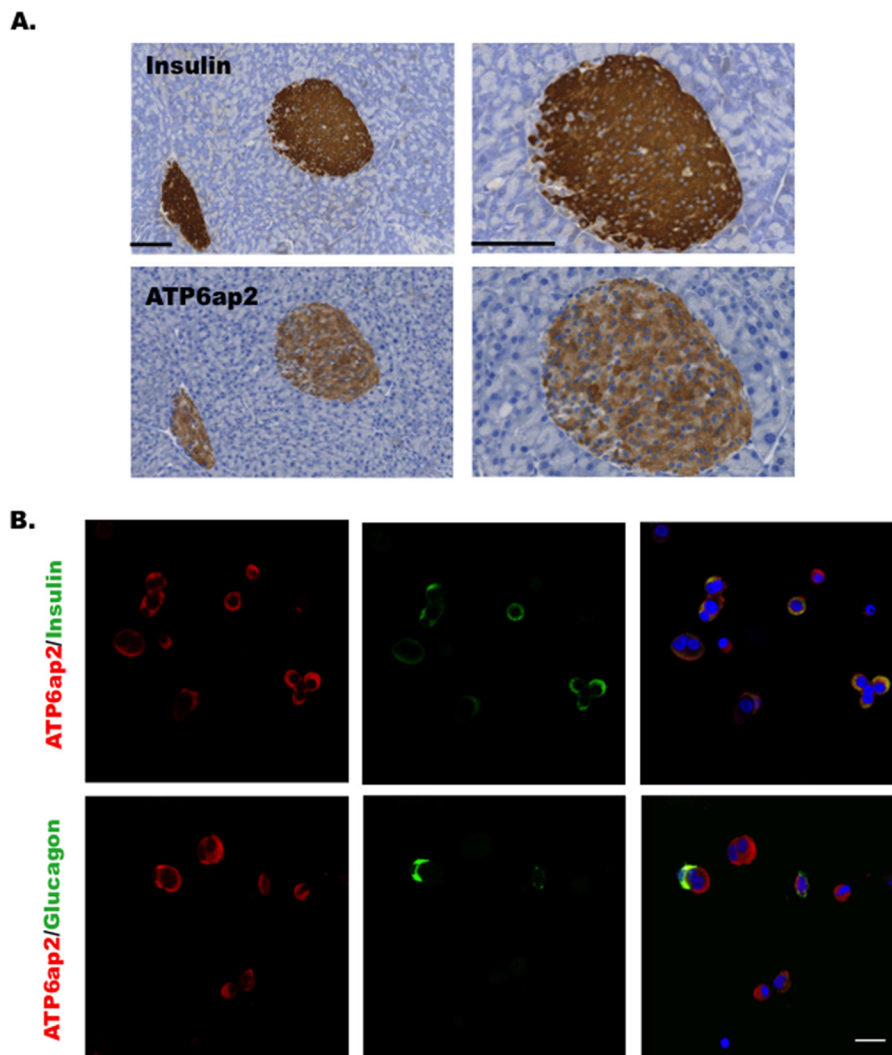


FIGURE 4. **ATP6ap2 expression in the pancreas and islets.** *A*, immunohistochemistry showing ATP6ap2 localization in the mouse pancreatic sections. The *right panels* show the enlarged images of the *left panels*. *Bar*, 100 μm . *B*, immunofluorescence showing ATP6ap2 localization in dispersed human islets. *Bar*, 20 μm . Representative images are from three independent experiments.

membrane-bound putative interactors in addition to ATP6ap2 and SELK found in our screens. Among the 13 interactors examined, ATP6ap2 was consistently the most abundant (Fig. 3) in all three cell types, whereas SELK was not. Some other membrane-bound interactors such as SYNGR4, APH1B, and GNAS showed only very low abundance compared with our control, Kcnj11, the subunit of the K_{ATP} channel required for glucose-stimulated insulin secretion (Fig. 3). The transcript expression profile pattern of these interactors was comparable among all three cell types, whereas only SLC39A7 and Leprotl1 had relatively higher expression levels compared with other interactors in mouse islets. Taken together, based on the expression pattern, ATP6ap2 identified from both islet MYTH screening was most highly expressed across all three cell types and was therefore chosen for further functional analysis.

ATP6ap2 has been shown to be expressed in several tissue including brain, heart, kidney, liver, pancreas, and adipose tissues (43, 44) with the highest levels reported in MIN6 cells (BioGPS (46, 47)). To localize ATP6ap2 expression within the pancreas, both immunohistochemistry and immunofluores-

cence staining were performed on mouse pancreatic slices and dispersed human islet cells, respectively. In mouse pancreata, ATP6ap2 was expressed in insulin immunopositive cells but not in acinar tissue (Fig. 4A). Further, in dispersed human islet cells, ATP6ap2 was shown to be expressed in both alpha and beta cells (Fig. 4B).

Interestingly, we found that the intensity of ATP6ap2 staining appeared weaker in islets from diabetic donors (Fig. 5A). The percentage of islet cells with strong fluorescence (>600 relative fluorescence intensity) decreased remarkably in diabetic islet cells compared with normal islet cells, whereas the percentage of those with weak fluorescence increased (Fig. 5A). These observations suggested decreased ATP6ap2 expression in diabetic islets. Further, we examined whether or not there was decreased expression in both alpha and beta cells. After co-staining with insulin or glucagon, we showed that ATP6ap2 expression was decreased primarily in beta cells (Fig. 5B). Importantly, correlating with ATP6ap2, islets from diabetic donors had impaired glucose-stimulated insulin secretion (GSIS) compared with controls (Fig. 5C).

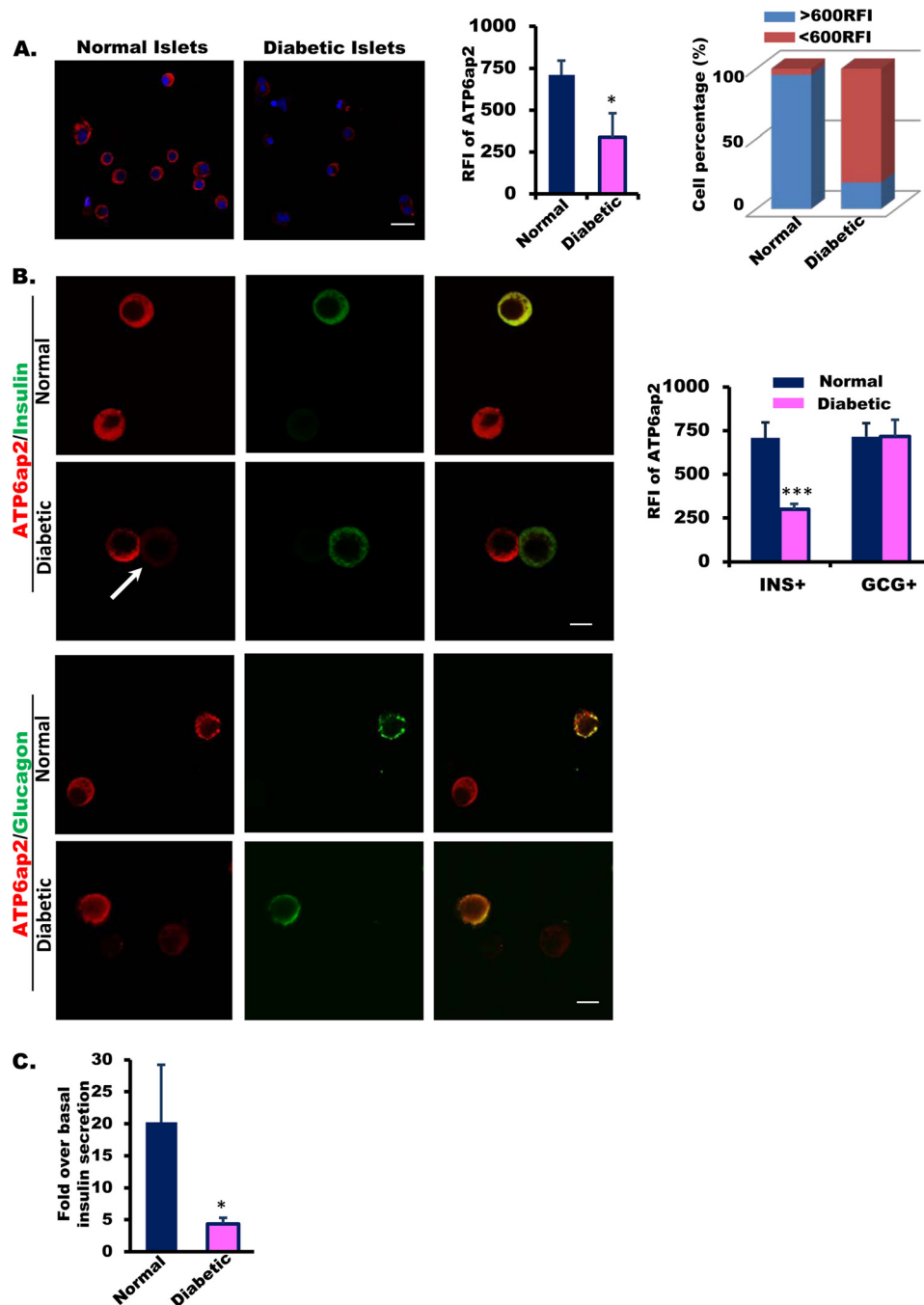


FIGURE 5. **ATP6ap2** expression and GSIS in human islets from normal and diabetic donors. *A*, representative images and quantitative analysis (quantification of fluorescence intensity and distribution of fluorescence intensity within cell population) of ATP6ap2 expression in human islets from normal and diabetic donors. *Bar*, 20 μ m. *B*, ATP6ap2 expression in human dispersed islets from diabetic donors. *Arrow* indicates reduced ATP6ap2 expression in insulin-positive cells. *Bar*, 10 μ m. Quantitative analysis of ATP6ap2 expression in both insulin- and glucagon-positive cells is shown (normal donors, $n = 3$; diabetic donors, $n = 2$). *C*, glucose-stimulated insulin secretion in human islets from diabetic donors.

Effect of Overexpressing ATP6ap2 on Insulin Secretion and cAMP Accumulation in INS-1 Cells—To further validate the interaction of GLP1R with ATP6ap2 employing the INS-1 cell line, we co-expressed epitope tagged GLP1R-V5 and ATP6ap2-FLAG. ATP6ap2 overexpression was detected using both anti-FLAG and anti-ATP6ap2 (Fig. 6A). GLP1R was detected after affinity purification of ATP6ap2-FLAG but not in GLP1R-expressing cell lysates alone, suggesting the interaction between two proteins in pancreatic beta cells (Fig. 6B) validating the MYTH assay results.

ATP6ap2 has been found to act as an adapter protein of the V-ATPase receptor complex (48) that maintains the acidic environment within vesicles required for the maturation and priming of insulin protein in pancreatic beta cells (49, 50). We further examined the effect of overexpressing ATP6ap2 in INS-1 cells. Interestingly, ATP6ap2 overexpression did not have any significant effect on insulin secretion under basal glucose conditions nor upon glucose or GLP1-induced insulin secretion (Fig. 6C) under the conditions studied. ATP6ap2 overexpression had no effect on GLP1-induced cAMP forma-

ATP6ap2 Regulates Insulin Secretion

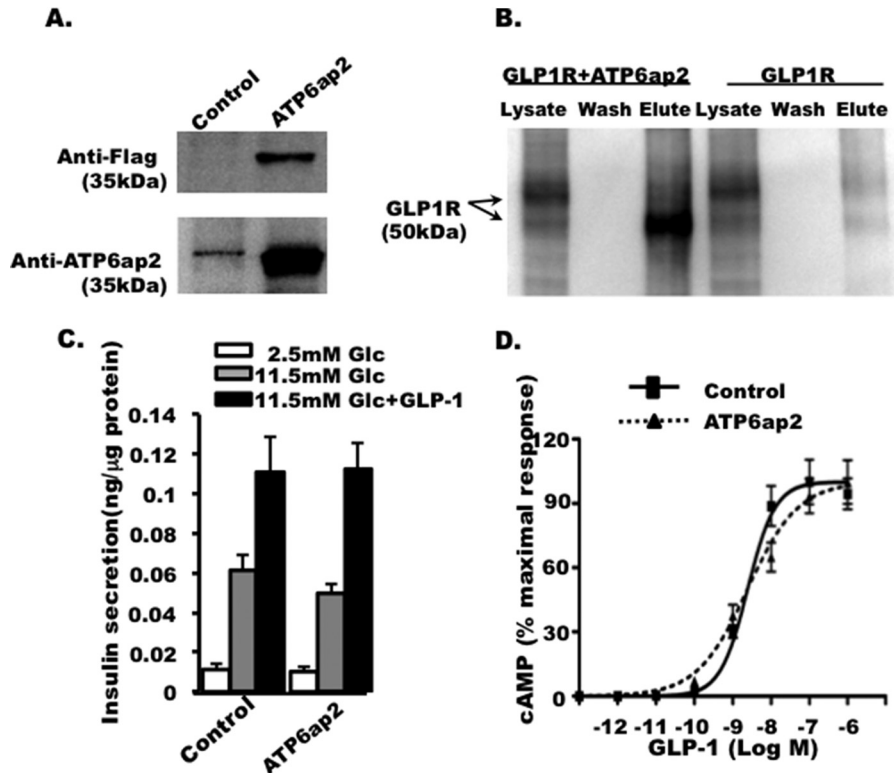


FIGURE 6. Effect of ATP6ap2 overexpression on insulin secretion and cAMP. *A*, overexpression of ATP6ap2, detected by anti-FLAG and anti-ATP6ap2. *B*, immunoprecipitation showing the interaction between GLP1R and ATP6ap2 in INS-1 cells. GLP1R overexpression alone was used as negative control to validate the specificity of immunoprecipitation. Representative images are from three independent experiments. *C*, effect of ATP6ap2 on glucose-stimulated insulin secretion in INS-1 cells. *D*, effect of ATP6ap2 overexpression on cAMP accumulation stimulated by GLP1 in CHO cells with GLP1R overexpressed.

tion (Fig. 6D), which is a key second messenger molecule in GLP1 signaling.

Effect of Knocking Down ATP6ap2 on Insulin Secretion and cAMP in INS-1 Cells—Because we did not observe significant effects in cells overexpressing ATP6ap2, to further elucidate the role of ATP6ap2 within pancreatic beta cells, we knocked down ATP6ap2 by siRNA (Fig. 7A). When ATP6ap2 was effectively knocked down (Fig. 7A), insulin secretion was decreased significantly under high glucose conditions (11.5 mM; Fig. 7B), as was GLP1-induced insulin secretion (Fig. 7B). This reduction in insulin secretion was not associated with cell death (data not shown) nor decreases in total insulin content (Fig. 7C). Furthermore, we showed that this attenuating effect only occurred at stimulatory glucose concentrations (11.5, 16.7, and 20 mM), not at low or moderate glucose levels (2.8 or 5.6 mM) (Fig. 7D). The inhibitory effect of ATP6ap2 knockdown was seen across a range of GLP1 concentrations (Fig. 7E).

GLP1R signaling effects are primarily mediated by the second messenger cAMP. In line with this, we found that down-regulation of ATP6ap2 led to a decrease in GLP1-stimulated cAMP accumulation in INS-1 cells (Fig. 7F). However, this effect was only observed at 0.1 and 10 nM GLP1 concentrations but not at a 1 μM GLP1 concentration (Fig. 7F), suggesting that the decrease in cAMP accumulation might be concentration-dependent. To confirm that the observation was specific, we also treated the siATP6ap2 transfected cells with forskolin (direct stimulation on adenylyl cyclase) and GIP (incretin acting on beta cells and sharing similar structure and signaling

pathways with GLP1R). We did not observe any difference in cAMP accumulation between control and ATP6ap2 knock-down cells (Fig. 7G). This suggested that down-regulation of ATP6ap2 specifically decreased GLP1R stimulated cAMP accumulation. The fact that we did not observe an ATP6ap2 effect in the overexpression model is likely due to the high abundance of native ATP6ap2 in INS-1 cells. Conversely, knocking down endogenous ATP6ap2 would likely exhibit more profound effects on the cells.

Effect of Knocking Down ATP6ap2 on Insulin Granule Morphology and Acidification—Because decreased insulin secretion and impaired insulin processing were observed in ATP6ap2 knockdown INS-1 cells, we next examined whether there were defects in insulin granule morphology using electron microscopy. We did not observe any change in granule morphology (Fig. 8A) or the number of insulin granules in siRNA treated INS1 cells (Fig. 8B), but the percentage of gray and empty granules was increased by more than 2-fold in ATP6ap2 knockdown cells (Fig. 8C). These results indicated that decreased insulin secretion was not due to the reduction of insulin granules *per se* but was possibly due to impaired insulin biosynthesis.

To further explore a processing defect, we detected an increased ratio of proinsulin *versus* insulin peptide in ATP6ap2 knockdown cells under all conditions including basal glucose, stimulated glucose, and GLP1 stimulation (Fig. 9A). This also suggested a possible impairment of insulin processing in ATP6ap2 knockdown cells. To address this, the expression of the prohormone convertases involved in insulin processing

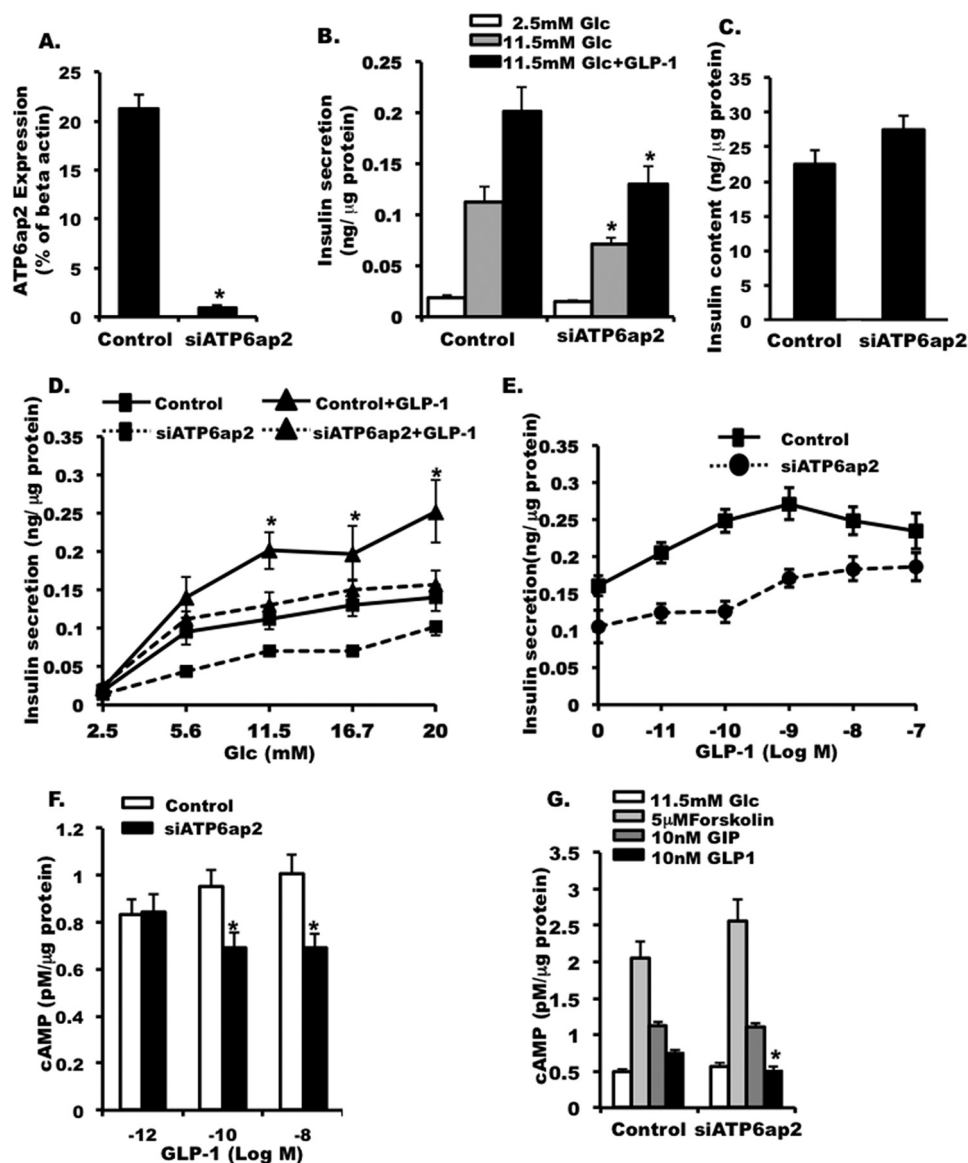


FIGURE 7. Effect of ATP6ap2 in INS-1 cells. *A*, qPCR showing the efficiency of siATP6ap2 in knocking down ATP6ap2 in INS-1 cells. *B*, effect of ATP6ap2 knockdown on insulin secretion in INS-1 cells. *C*, insulin content in INS-1 cells transfected with siATP6ap2. *D*, insulin secretion in INS-1 cells transfected with scrambled siRNA (*Control*) and siATP6ap2 at different glucose concentration. *E*, insulin secretion in cells transfected with siATP6ap2 at 11.5 mM glucose in the presence of incremental doses of GLP1. *F*, cAMP accumulation in INS-1 cells transfected with siATP6ap2 at different doses of GLP1. *G*, cAMP accumulation in siATP6ap2 transfected cells that were treated with forskolin, GIP, and GLP1, respectively. The values are represented by the averages \pm S.E. from triplicates in at least three independent experiments. *, $p < 0.05$ ($n = 4-6$).

including PC1/3, PC2, and CPE (51–55) were examined. There was no difference in the transcript expression of these three key enzymes (Fig. 9B), suggesting that other factors are contributing to impaired insulin processing. It was reported that acidification within insulin granules was critical for their maturation and priming (56). To examine whether ATP6ap2 is involved in the acidification of the insulin granules, we loaded the cells with acidotropic LysoTracker, a dye that accumulates specifically in acidic organelles. In pancreatic beta cells, the majority of cellular acidic structures are indeed insulin granules; therefore LysoTracker staining can be used to evaluate the acidity of the granule given the fact that insulin granule number did not change in ATP6ap2 knockdown cells compared with the control (Fig. 8B). Consistent with previous studies (57), the cells treated with V-ATPase inhibitor bafilomycin were barely stained with Lyso-

Tracker, suggesting that granule acidification was blocked (Fig. 9C). Similarly, LysoTracker staining in ATP6ap2 knockdown cells was shown to be decreased significantly when compared with control cells, suggesting that insulin granule acidification was impaired (Fig. 9C). Taken together, these results suggest that decreased insulin processing and secretion upon ATP6ap2 knockdown could be due to impairment of acidification within individual insulin granules.

ATP6ap2 Effects on GLP1-stimulated Ca^{2+} Influx—GLP1 R activation increases intracellular Ca^{2+} mediated by PKA and Epac (cAMP) (26, 58). We observed a robust increase in intracellular Ca^{2+} in control dispersed mouse islets upon GLP1 stimulation (Fig. 10A, upper two panels). However, when we knock down ATP6ap2 in dispersed islet cells (Fig. 10B), the GLP1-induced increase in Ca^{2+} was completely diminished,

ATP6ap2 Regulates Insulin Secretion

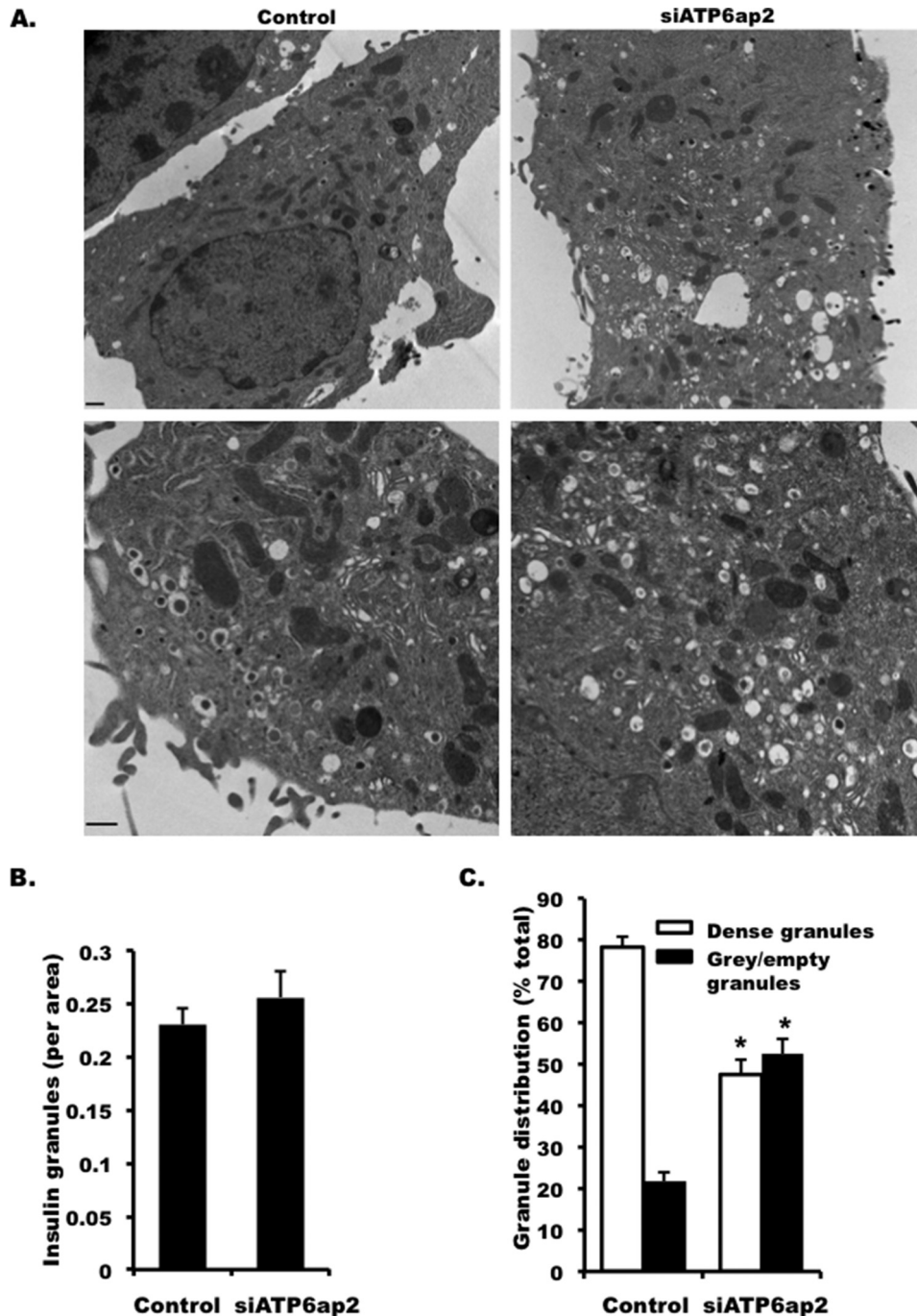


FIGURE 8. Effect of knocking down ATP6ap2 on insulin granules. *A*, representative images of electron microscopy showing insulin granules in INS-1 cells transfected with siATP6ap2. The *lower panel* is shown in higher magnification. *Bar*, 500 nm. *B*, granule numbers in INS-1 cells transfected with siATP6ap2. *C*, percentages of dense (mature) and gray/empty (immature) granules in INS-1 cells transfected with siATP6ap2. Representative images are from at least three independent experiments. *, $p < 0.05$ ($n = 3-5$).

suggesting that ATP6ap2 was required for GLP1-induced Ca^{2+} influx (Fig. 10A, *lower two panels*).

Discussion

The GLP1R and its associated signaling pathways have gained much attention over the past several years because they are targets for current and future medications to treat type 2 diabetes. In this study, we have used a novel MYTH assay (Fig. 1) to screen mouse and human islet cDNA libraries, enabling us to discover over 50 novel putative interactors of GLP1R. Each of

these interactors has the potential to regulate pancreatic beta cell function through GLP1R. The interactor, ATP6ap2, was identified in both mouse and human islet screens and pursued in further studies because of its consistently high expression across beta cell lines and primary islets. Our results showed that ATP6ap2 plays an important dual role; first, it regulates GLP1R signaling through cAMP, and second, it likely facilitates the processing of insulin through granule acidification. We realize that the latter effect appears GLP-1R-independent and may be a more global permissive effect of ATP6ap2 on insulin secre-

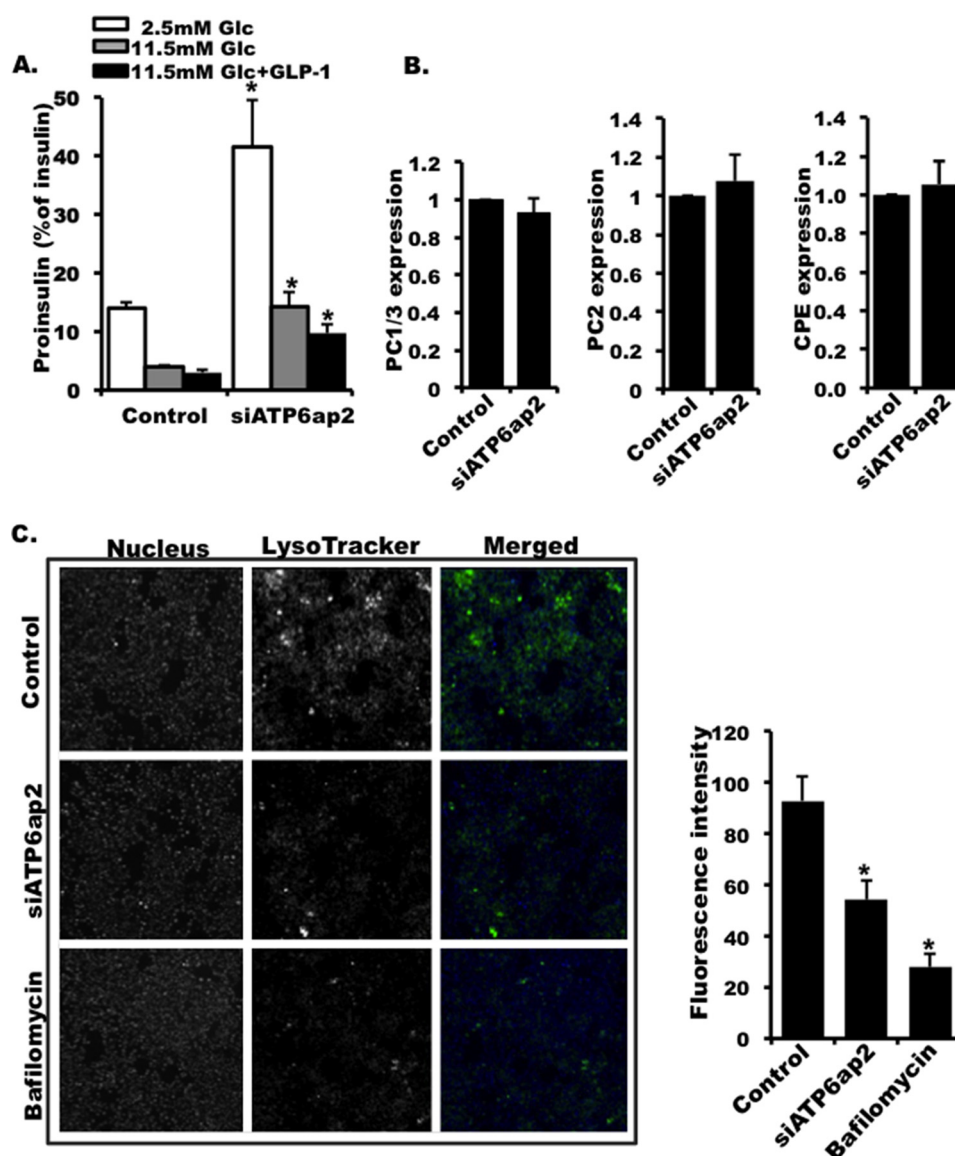


FIGURE 9. Effect of knocking down ATP6ap2 on insulin granule acidification and proinsulin processing. *A*, ratio of proinsulin versus insulin in cells transfected with siATP6ap2. *B*, expression of PC1/3, PC2, and CPE in INS-1 cells transfected with siATP6ap2. The expression was presented as ratio over control. *C*, representative images and quantitative analysis of LysoTracker staining of INS1 cells transfected with scramble siRNA (control), siATP6ap2, and treated with bafilomycin A (10 nM). The values are represented by the averages \pm S.E. from triplicates in three independent experiments. *, $p < 0.05$ ($n = 3$).

tion. Future studies will further delineate the mechanistic link between GLP1R signaling and more general permissive beta cell effects.

In this study, we chose to identify potential interactors of GLP1R from MYTH screens on mouse and human islet cDNA libraries. Previous studies conducted by us have focused on a human fetal brain cDNA library, using a similar approach. However, we reasoned that pancreatic islet tissue is a more appropriate model from which to screen for interactors of GLP1R with the intension of understanding GLP1R signaling in the beta cell specifically. The pancreatic islet consists of a composition of cells including beta, alpha, and delta cells; however, the expression pattern of GLP1R predominantly in beta cells has been widely accepted (19–21), much less in alpha or delta cells (21). However, it is possible that other glucagon receptor subfamily or GPCR interactors that normally are not found in

GLP1R-expressing cells may in islet tissue interact with GLP1R, requiring rigorous testing for specificity. Notwithstanding this possibility, the pancreatic islet appears to be a good model tissue in which to study the GLP1R interactome in a beta cell specific setting.

Our study was able to identify a series of novel interactors involved in a variety of intracellular functions (Fig. 2), supporting the dynamic role that GLP1R plays in the regulation of pancreatic beta cell function. Of the common interactors identified from both mouse and human islet screens, the interactor ATP6ap2 was expressed at abundant levels in MIN6, INS-1, and mouse islets. Furthermore, by immunohistochemistry in mouse pancreatic sections, we showed that ATP6ap2 was expressed in endocrine islets but not acinar cells (Fig. 4A). Further analysis on human dispersed islets revealed ATP6ap2 expression in both pancreatic beta and alpha cells (Fig. 4B).

ATP6ap2 Regulates Insulin Secretion

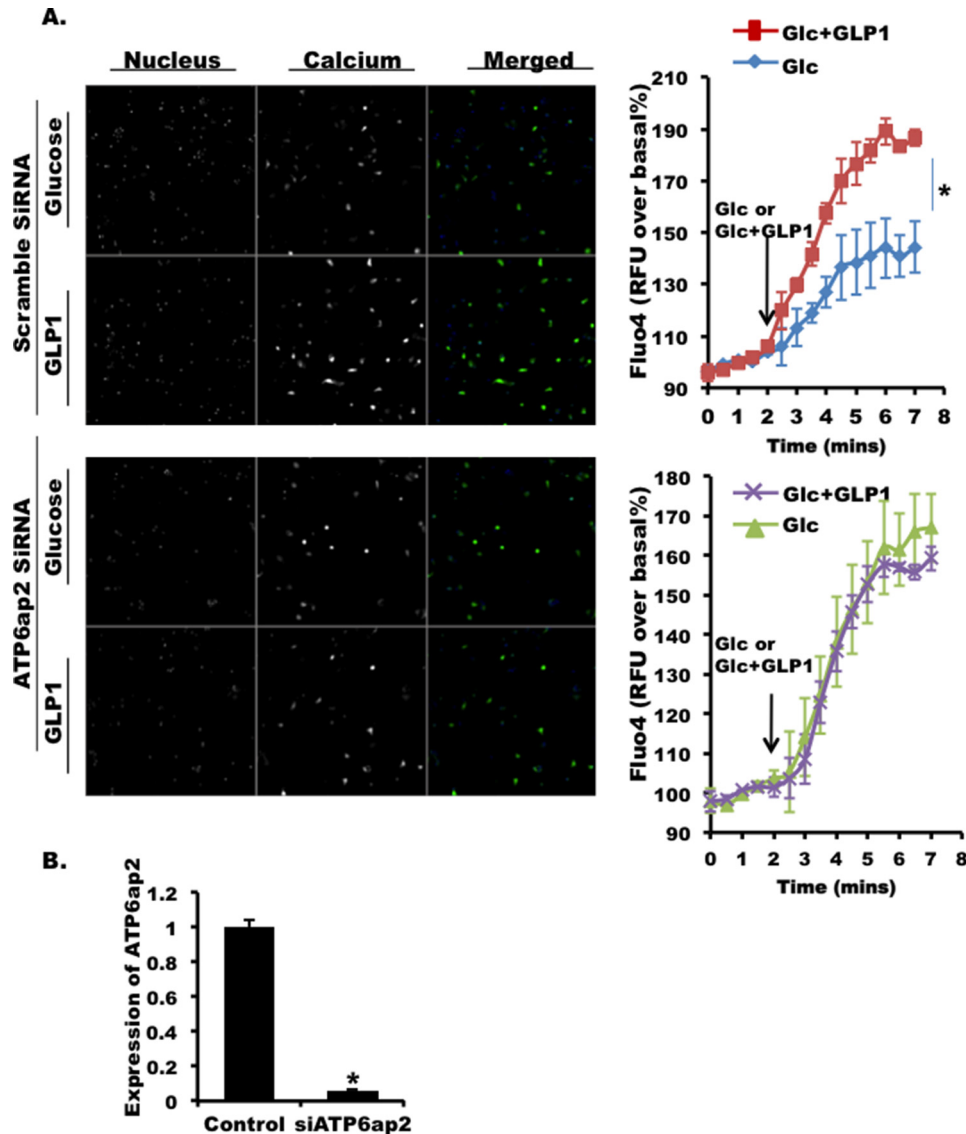


FIGURE 10. **Effect of ATP6ap2 knockdown on intracellular Ca^{2+} in dispersed mouse islets.** A, representative images (5 min after GLP1 stimulation) and quantitative analysis of Fluo4 in dispersed mouse islets transfected with scramble siRNA (control, upper panels) or siATP6ap2 (lower panels). Nuclear staining in blue and Fluo4 in green for merged images. B, qPCR showing the efficiency of ATP6ap2 knockdown in dispersed mouse islets. The values are represented by the averages \pm S.E. from triplicates in three independent experiments. *, $p < 0.05$ ($n = 3$).

ATP6ap2 is known as an accessory protein of the V-ATPase (59) composed of a transmembrane proton-translocation domain (V_0) and extramembrane pump domain (V_1 sectors) (60). Although there is no direct evidence demonstrating the effect of ATP6ap2 on insulin secretion in pancreatic beta cells, previous studies have demonstrated that the ATP6 V_0 B subunit of V-ATPase increased 2.38-fold in human diabetic *versus* normal islets by microarray analysis (61). Also, the islet tropic $\alpha 3$ isoform (membrane-intrinsic subunit) of V-ATPase was reported to regulate insulin secretion from pancreatic beta cells (12). We observed reduced expression of ATP6ap2 in human diabetic *versus* normal islets, and the reduction was not in alpha but beta cells (Fig. 5). The reduced expression of ATP6ap2 was accompanied by an impaired GSIS in the human diabetic islets. In line with these observations, we showed that the down-regulation of ATP6ap2 resulted in decreased GSIS and GLP1-induced insulin secretion, suggesting a regulatory role of

ATP6ap2 in insulin secretion from pancreatic beta cells. cAMP-PKA is an important pathway for GLP1-induced insulin secretion, and V-ATPase is required for the full activation of PKA in response to glucose stimulation (14). In our studies, cAMP accumulation was significantly decreased at GLP1 concentrations of 0.1 and 10 nM but not at 1 pM, and this effect was not observed in forskolin- or GIP-treated cells (Fig. 7G), suggesting that the cAMP-PKA pathway might be involved in GLP1-induced insulin secretion. The downstream molecules of cAMP are PKA and Epac. Because GLP1R activation increases intracellular Ca^{2+} via PKA and Epac (26, 58), one would expect ATP6ap2 knockdown could affect Ca^{2+} influx associated with GLP1. Indeed, we found that the GLP1-induced increase in Ca^{2+} was abolished in ATP6ap2 knockdown cells, suggesting a requirement of ATP6ap2 for GLP1R Ca^{2+} signaling. This could also in part explain the decreased insulin secretion in cells with ATP6ap2 knocked down.

ATP6ap2 has been shown to be involved in the maintenance of acidity within secretory vesicles (62). Previously, it was demonstrated that whole body knock-out of ATP6ap2 was lethal in mice (63); whereas, tissue specific knock-out studies of ATP6ap2 in cardiomyocytes or in podocytes resulted in detrimental defects after birth including heart failure or renal failure, respectively (64, 65). These studies confirmed the requirement of ATP6ap2 association with V-ATPase, as well as the functional role of ATP6ap2 in maintaining the acidity of microenvironments within intracellular vesicles. Previous studies have shown the involvement of acidic secretory vesicles in insulin processing and maturation (66). Specifically, proprotein convertases 3 (PC1/3) and 2 (PC2) responsible for insulin processing from proinsulin are strictly pH-dependent (51, 67). In line with this, the gene expression of insulin-processing enzymes PC1/3, PC2, and CPE were not changed in ATP6ap2 knockdown cells. However, granule acidification was impaired, causing increased pH, which might inhibit the activity of the insulin-processing enzymes. Furthermore, an increased proinsulin *versus* insulin ratio was detected, suggesting impairment in insulin processing and maturation within secretory vesicles from ATP6ap2 knockdown cells. To support this, we observed reduced expression of ATP6ap2 in islets from type 2 diabetic donors, whose GSIS was largely decreased. Our data provided a link between ATP6ap2 and diabetes where loss of ATP6ap2 impaired insulin processing via increasing granule pH.

In summary, our study provided a novel insight into GLP1R signaling and was the first to identify GLP1R interactors in pancreatic islets. Our data also suggested that these interacting proteins of GLP1R could be involved in the regulation of insulin secretion and GLP1R signaling in pancreatic beta cells. Because GLP1R has been used as potent drug target in the treatment of diabetes, our findings could contribute to the development of novel effective therapeutic strategies for this disease.

Author Contributions—F. F. D. designed experiments and analyzed the data, coordinated the study, and wrote the paper. A. B., Y. L., B. B., X. W., and M. Z. contributed to the acquisition of data, analysis, and interpretation of data. X. H., L. L., D. Z., and H. G. provided technical assistance with specific studies and contributed to the preparation of relevant figures. M. B. W. designed the overall study. All authors reviewed the results and approved the final version of the manuscript submitted.

Acknowledgments—We thank both the Alberta Islet Distribution Program and the Alberta Diabetes Institute IsletCore at the University of Alberta (with the assistance of the Human Organ Procurement and Exchange Program and the Trillium Gift of Life Network in the procurement of donor pancreata for research) for generously providing human islets.

References

- Drucker, D. J., and Nauck, M. A. (2006) The incretin system: glucagon-like peptide-1 receptor agonists and dipeptidyl peptidase-4 inhibitors in type 2 diabetes. *Lancet* **368**, 1696–1705
- Edwards, C. M., Todd, J. F., Mahmoudi, M., Wang, Z., Wang, R. M., Ghatei, M. A., and Bloom, S. R. (1999) Glucagon-like peptide 1 has a physiological role in the control of postprandial glucose in humans: studies with the antagonist exendin 9–39. *Diabetes* **48**, 86–93
- Kreymann, B., Williams, G., Ghatei, M. A., and Bloom, S. R. (1987) Glucagon-like peptide-1 7–36: a physiological incretin in man. *Lancet* **2**, 1300–1304
- Salehi, M., Vahl, T. P., and D'Alessio, D. A. (2008) Regulation of islet hormone release and gastric emptying by endogenous glucagon-like peptide 1 after glucose ingestion. *J. Clin. Endocrinol. Metab.* **93**, 4909–4916
- Woerle, H. J., Carneiro, L., Derani, A., Göke, B., and Schirra, J. (2012) The role of endogenous incretin secretion as amplifier of glucose-stimulated insulin secretion in healthy subjects and patients with type 2 diabetes. *Diabetes* **61**, 2349–2358
- Boutant, M., Ramos, O. H., Tourrel-Cuzin, C., Movassat, J., Ilias, A., Vallois, D., Planchais, J., Pégrier, J. P., Schuit, F., Petit, P. X., Bossard, P., Maedler, K., Grapin-Botton, A., and Vasseur-Cognet, M. (2012) COUP-TFII controls mouse pancreatic β -cell mass through GLP-1- β -catenin signaling pathways. *PLoS One* **7**, e30847
- Heller, C., Kühn, M. C., Mülders-Opgenoorth, B., Schott, M., Willenberg, H. S., Scherbaum, W. A., and Schinner, S. (2011) Exendin-4 upregulates the expression of Wnt-4, a novel regulator of pancreatic β -cell proliferation. *Am. J. Physiol. Endocrinol. Metab.* **301**, E864–E872
- Liu, Z., and Habener, J. F. (2008) Glucagon-like peptide-1 activation of TCF7L2-dependent Wnt signaling enhances pancreatic β cell proliferation. *J. Biol. Chem.* **283**, 8723–8735
- Ye, Y., Keyes, K. T., Zhang, C., Perez-Polo, J. R., Lin, Y., and Birnbaum, Y. (2010) The myocardial infarct size-limiting effect of sitagliptin is PKA-dependent, whereas the protective effect of pioglitazone is partially dependent on PKA. *Am. J. Physiol. Heart Circ. Physiol.* **298**, H1454–H1465
- Sokos, G. G., Nikolaidis, L. A., Mankad, S., Elahi, D., and Shannon, R. P. (2006) Glucagon-like peptide-1 infusion improves left ventricular ejection fraction and functional status in patients with chronic heart failure. *J. Card. Fail.* **12**, 694–699
- Krisai, P., Aeschbacher, S., Schoen, T., Bossard, M., van der Stouwe, J. G., Dörig, L., Todd, J., Estis, J., Risch, M., Risch, L., and Conen, D. (2015) Glucagon-like peptide-1 and blood pressure in young and healthy adults from the general population. *Hypertension* **65**, 306–312
- Hirata, K., Kume, S., Araki, S., Sakaguchi, M., Chin-Kanasaki, M., Isshiki, K., Sugimoto, T., Nishiyama, A., Koya, D., Haneda, M., Kashiwagi, A., and Uzu, T. (2009) Exendin-4 has an anti-hypertensive effect in salt-sensitive mice model. *Biochem. Biophys. Res. Commun.* **380**, 44–49
- von Scholten, B. J., Lajer, M., Goetze, J. P., Persson, F., and Rossing, P. (2015) Time course and mechanisms of the anti-hypertensive and renal effects of liraglutide treatment. *Diabet. Med.* **32**, 343–352
- Yu, M., Moreno, C., Hoagland, K. M., Dahly, A., Ditter, K., Mistry, M., and Roman, R. J. (2003) Antihypertensive effect of glucagon-like peptide 1 in Dahl salt-sensitive rats. *J. Hypertens.* **21**, 1125–1135
- During, M. J., Cao, L., Zuzga, D. S., Francis, J. S., Fitzsimons, H. L., Jiao, X., Bland, R. J., Klugmann, M., Banks, W. A., Drucker, D. J., and Haile, C. N. (2003) Glucagon-like peptide-1 receptor is involved in learning and neuroprotection. *Nat. Med.* **9**, 1173–1179
- Hamilton, A., Patterson, S., Porter, D., Gault, V. A., and Holscher, C. (2011) Novel GLP-1 mimetics developed to treat type 2 diabetes promote progenitor cell proliferation in the brain. *J. Neurosci. Res.* **89**, 481–489
- Hunter, K., and Hölscher, C. (2012) Drugs developed to treat diabetes, liraglutide and lixisenatide, cross the blood brain barrier and enhance neurogenesis. *BMC Neurosci.* **13**, 33
- Dillon, J. S., Tanizawa, Y., Wheeler, M. B., Leng, X. H., Ligon, B. B., Rabin, D. U., Yoo-Warren, H., Permutt, M. A., and Boyd, A. E., 3rd (1993) Cloning and functional expression of the human glucagon-like peptide-1 (GLP-1) receptor. *Endocrinology* **133**, 1907–1910
- Jun, L. S., Showalter, A. D., Ali, N., Dai, F., Ma, W., Coskun, T., Ficorilli, J. V., Wheeler, M. B., Michael, M. D., and Sloop, K. W. (2014) A novel humanized GLP-1 receptor model enables both affinity purification and Cre-LoxP deletion of the receptor. *PLoS. One* **9**, e93746
- Pyke, C., Heller, R. S., Kirk, R. K., Ørskov, C., Reedtz-Runge, S., Kaastrup, P., Hvelplund, A., Bardram, L., Calatayud, D., and Knudsen, L. B. (2014) GLP-1 receptor localization in monkey and human tissue: novel distribution revealed with extensively validated monoclonal antibody. *Endocrinology* **155**, 1280–1290
- Richards, P., Parker, H. E., Adriaenssens, A. E., Hodgson, J. M., Cork, S. C.,

ATP6ap2 Regulates Insulin Secretion

- Trapp, S., Gribble, F. M., and Reimann, F. (2014) Identification and characterization of GLP-1 receptor-expressing cells using a new transgenic mouse model. *Diabetes* **63**, 1224–1233
22. Gromada, J., Holst, J. J., and Rorsman, P. (1998) Cellular regulation of islet hormone secretion by the incretin hormone glucagon-like peptide 1. *Pflugers Arch.* **435**, 583–594
23. Wheeler, M. B., Lu, M., Dillon, J. S., Leng, X. H., Chen, C., and Boyd, A. E. III (1993) Functional expression of the rat glucagon-like peptide-1 receptor, evidence for coupling to both adenylyl cyclase and phospholipase-C. *Endocrinology* **133**, 57–62
24. Seino, S., and Shibasaki, T. (2005) PKA-dependent and PKA-independent pathways for cAMP-regulated exocytosis. *Physiol. Rev.* **85**, 1303–1342
25. Gromada, J., Bokvist, K., Ding, W. G., Holst, J. J., Nielsen, J. H., and Rorsman, P. (1998) Glucagon-like peptide 1 (7–36) amide stimulates exocytosis in human pancreatic β -cells by both proximal and distal regulatory steps in stimulus-secretion coupling. *Diabetes* **47**, 57–65
26. Kang, G., Chepurny, O. G., and Holz, G. G. (2001) cAMP-regulated guanine nucleotide exchange factor II (Epac2) mediates Ca^{2+} -induced Ca^{2+} release in INS-1 pancreatic β -cells. *J. Physiol.* **536**, 375–385
27. Buteau, J., Foisy, S., Rhodes, C. J., Carpenter, L., Biden, T. J., and Prentki, M. (2001) Protein kinase Czeta activation mediates glucagon-like peptide-1-induced pancreatic β -cell proliferation. *Diabetes* **50**, 2237–2243
28. Buteau, J., Foisy, S., Joly, E., and Prentki, M. (2003) Glucagon-like peptide 1 induces pancreatic β -cell proliferation via transactivation of the epidermal growth factor receptor. *Diabetes* **52**, 124–132
29. Bockaert, J., Fagni, L., Dumuis, A., and Marin, P. (2004) GPCR interacting proteins (GIP). *Pharmacol. Ther.* **103**, 203–221
30. Schwenk, J., Metz, M., Zolles, G., Turecek, R., Fritzius, T., Bildl, W., Tarusawa, E., Kulik, A., Unger, A., Ivankova, K., Seddik, R., Tiao, J. Y., Rajalu, M., Trojanova, J., Rohde, V., Gassmann, M., Schulte, U., Fakler, B., and Bettler, B. (2010) Native GABA_B receptors are heteromultimers with a family of auxiliary subunits. *Nature* **465**, 231–235
31. Sonoda, N., Imamura, T., Yoshizaki, T., Babendure, J. L., Lu, J. C., and Olefsky, J. M. (2008) β -Arrestin-1 mediates glucagon-like peptide-1 signaling to insulin secretion in cultured pancreatic β cells. *Proc. Natl. Acad. Sci. U.S.A.* **105**, 6614–6619
32. Syme, C. A., Zhang, L., and Bisello, A. (2006) Caveolin-1 regulates cellular trafficking and function of the glucagon-like peptide 1 receptor. *Mol. Endocrinol.* **20**, 3400–3411
33. Talbot, J., Joly, E., Prentki, M., and Buteau, J. (2012) β -Arrestin1-mediated recruitment of c-Src underlies the proliferative action of glucagon-like peptide-1 in pancreatic β INS832/13 cells. *Mol. Cell Endocrinol.* **364**, 65–70
34. Huang, X., Dai, F. F., Gaisano, G., Giglou, K., Han, J., Zhang, M., Kittanokom, S., Wong, V., Wei, L., Showalter, A. D., Sloop, K. W., Stagljar, I., and Wheeler, M. B. (2013) The identification of novel proteins that interact with the GLP-1 receptor and restrain its activity. *Mol. Endocrinol.* **27**, 1550–1563
35. Joseph, J. W., Koshkin, V., Saleh, M. C., Sivitz, W. I., Zhang, C. Y., Lowell, B. B., Chan, C. B., and Wheeler, M. B. (2004) Free fatty acid-induced β -cell defects are dependent on uncoupling protein 2 expression. *J. Biol. Chem.* **279**, 51049–51056
36. Liu, Y., Batchuluun, B., Ho, L., Zhu, D., Prentice, K. J., Bhattacharjee, A., Zhang, M., Pourasgari, F., Hardy, A. B., Taylor, K. M., Gaisano, H., Dai, F. F., and Wheeler, M. B. (2015) Characterization of zinc influx transporters (ZIPs) in pancreatic β cells: roles in regulating cytosolic zinc homeostasis and insulin secretion. *J. Biol. Chem.* **290**, 18757–18769
37. Wolff, N. A., Ghio, A. J., Garrick, L. M., Garrick, M. D., Zhao, L., Fenton, R. A., and Thévenod, F. (2014) Evidence for mitochondrial localization of divalent metal transporter 1 (DMT1). *FASEB J.* **28**, 2134–2145
38. Dünwald, M., Varshavsky, A., and Johnsson, N. (1999) Detection of transient *in vivo* interactions between substrate and transporter during protein translocation into the endoplasmic reticulum. *Mol. Biol. Cell* **10**, 329–344
39. Johnsson, N., and Varshavsky, A. (1994) Ubiquitin-assisted dissection of protein transport across membranes. *EMBO J.* **13**, 2686–2698
40. Stagljar, I., Korostensky, C., Johnsson, N., and te Heesen, S. (1998) A genetic system based on split-ubiquitin for the analysis of interactions between membrane proteins *in vivo*. *Proc. Natl. Acad. Sci. U.S.A.* **95**, 5187–5192
41. Wittke, S., Lewke, N., Müller, S., and Johnsson, N. (1999) Probing the molecular environment of membrane proteins *in vivo*. *Mol. Biol. Cell* **10**, 2519–2530
42. Dai, F. F., Zhang, Y., Kang, Y., Wang, Q., Gaisano, H. Y., Braunewell, K. H., Chan, C. B., and Wheeler, M. B. (2006) The neuronal Ca^{2+} sensor protein visinin-like protein-1 is expressed in pancreatic islets and regulates insulin secretion. *J. Biol. Chem.* **281**, 21942–21953
43. Zhang, M., Robitaille, M., Showalter, A. D., Huang, X., Liu, Y., Bhattacharjee, A., Willard, F. S., Han, J., Froese, S., Wei, L., Gaisano, H. Y., Angers, S., Sloop, K. W., Dai, F. F., and Wheeler, M. B. (2014) Progesterone receptor membrane component 1 is a functional part of the glucagon-like peptide-1 (GLP-1) receptor complex in pancreatic β cells. *Mol. Cell Proteomics* **13**, 3049–3062
44. Wijesekara, N., Dai, F. F., Hardy, A. B., Giglou, P. R., Bhattacharjee, A., Koshkin, V., Chimienti, F., Gaisano, H. Y., Rutter, G. A., and Wheeler, M. B. (2010) β Cell-specific Znt8 deletion in mice causes marked defects in insulin processing, crystallisation and secretion. *Diabetologia* **53**, 1656–1668
45. Lu, H., Koshkin, V., Allister, E. M., Gyulkhandanyan, A. V., and Wheeler, M. B. (2010) Molecular and metabolic evidence for mitochondrial defects associated with β -cell dysfunction in a mouse model of type 2 diabetes. *Diabetes* **59**, 448–459
46. Wu, C., Orozco, C., Boyer, J., Leglise, M., Goodale, J., Batalov, S., Hodge, C. L., Haase, J., Janes, J., Huss, J. W., 3rd, and Su, A. I. (2009) BioGPS: an extensible and customizable portal for querying and organizing gene annotation resources. *Genome Biol.* **10**, R130
47. Wu, C., Macleod, I., and Su, A. I. (2013) BioGPS and MyGene.info: organizing online, gene-centric information. *Nucleic Acids Res.* **41**, D561–D565
48. Jansen, E. J., and Martens, G. J. (2012) Novel insights into V-ATPase functioning: distinct roles for its accessory subunits ATP6AP1/Ac45 and ATP6AP2/(pro) renin receptor. *Curr. Protein Pept. Sci.* **13**, 124–133
49. Forgas, M. (2007) Vacuolar ATPases: rotary proton pumps in physiology and pathophysiology. *Nat. Rev. Mol. Cell Biol.* **8**, 917–929
50. Marshansky, V., and Futai, M. (2008) The V-type H⁺-ATPase in vesicular trafficking: targeting, regulation and function. *Curr. Opin. Cell Biol.* **20**, 415–426
51. Smeeckens, S. P., Montag, A. G., Thomas, G., Albiges-Rizo, C., Carroll, R., Benig, M., Phillips, L. A., Martin, S., Ohagi, S., and Gardner, P., (1992) Proinsulin processing by the subtilisin-related proprotein convertases furin, PC2, and PC3. *Proc. Natl. Acad. Sci. U.S.A.* **89**, 8822–8826
52. Muller, L., and Lindberg, I. (1999) The cell biology of the prohormone convertases PC1 and PC2. *Prog. Nucleic Acids Res. Mol. Biol.* **63**, 69–108
53. Naggert, J. K., Fricker, L. D., Varlamov, O., Nishina, P. M., Rouille, Y., Steiner, D. F., Carroll, R. J., Paigen, B. J., and Leiter, E. H. (1995) Hyperproinsulinaemia in obese fat/fat mice associated with a carboxypeptidase E mutation which reduces enzyme activity. *Nat. Genet.* **10**, 135–142
54. Seidah, N. G., Mowla, S. J., Hamelin, J., Mamarbachi, A. M., Benjannet, S., Touré, B. B., Basak, A., Munzer, J. S., Marcinkiewicz, J., Zhong, M., Barale, J. C., Lazure, C., Murphy, R. A., Chrétien, M., and Marcinkiewicz, M. (1999) Mammalian subtilisin/kexin isozyme SKI-1: A widely expressed proprotein convertase with a unique cleavage specificity and cellular localization. *Proc. Natl. Acad. Sci. U.S.A.* **96**, 1321–1326
55. Zhu, X., Orci, L., Carroll, R., Norrbom, C., Ravazzola, M., and Steiner, D. F. (2002) Severe block in processing of proinsulin to insulin accompanied by elevation of des-64,65 proinsulin intermediates in islets of mice lacking prohormone convertase 1/3. *Proc. Natl. Acad. Sci. U.S.A.* **99**, 10299–10304
56. Rorsman, P., Eliasson, L., Renström, E., Gromada, J., Barg, S., and Göpel, S. (2000) The cell physiology of biphasic insulin secretion. *News Physiol. Sci.* **15**, 72–77
57. Sun-Wada, G. H., Toyomura, T., Murata, Y., Yamamoto, A., Futai, M., and Wada, Y. (2006) The $\alpha 3$ isoform of V-ATPase regulates insulin secretion from pancreatic β -cells. *J. Cell Sci.* **119**, 4531–4540
58. Tsuboi, T., da, Silva, X., Holz, G. G., Jouaville, L. S., Thomas, A. P., and Rutter, G. A. (2003) Glucagon-like peptide-1 mobilizes intracellular Ca^{2+}

- and stimulates mitochondrial ATP synthesis in pancreatic MIN6 β -cells. *Biochem. J.* **369**, 287–299
59. Ludwig, J., Kerscher, S., Brandt, U., Pfeiffer, K., Getlawi, F., Apps, D. K., and Schägger, H. (1998) Identification and characterization of a novel 9.2-kDa membrane sector-associated protein of vacuolar proton-ATPase from chromaffin granules. *J. Biol. Chem.* **273**, 10939–10947
 60. Cruciat, C. M., Ohkawara, B., Acebron, S. P., Karaulanov, E., Reinhard, C., Ingelfinger, D., Boutros, M., and Niehrs, C. (2010) Requirement of prorenin receptor and vacuolar H⁺-ATPase-mediated acidification for Wnt signaling. *Science* **327**, 459–463
 61. Gunton, J. E., Kulkarni, R. N., Yim, S., Okada, T., Hawthorne, W. J., Tseng, Y. H., Roberson, R. S., Ricordi, C., O'Connell, P. J., Gonzalez, F. J., and Kahn, C. R. (2005) Loss of ARNT/HIF1 β mediates altered gene expression and pancreatic-islet dysfunction in human type 2 diabetes. *Cell* **122**, 337–349
 62. Riediger, F., Quack, I., Qadri, F., Hartleben, B., Park, J. K., Potthoff, S. A., Sohn, D., Sihn, G., Rousselle, A., Fokuhl, V., Maschke, U., Purfürst, B., Schneider, W., Rump, L. C., Luft, F. C., Dechend, R., Bader, M., Huber, T. B., Nguyen, G., and Muller, D. N. (2011) Prorenin receptor is essential for podocyte autophagy and survival. *J. Am. Soc. Nephrol.* **12**, 2193–2202
 63. Sihn, G., Rousselle, A., Vilianovitch, L., Burckle, C., and Bader, M. (2010) Physiology of the (pro)renin receptor: Wnt of change? *Kidney Int.* **78**, 246–256
 64. Kinouchi, K., Ichihara, A., Sano, M., Sun-Wada, G. H., Wada, Y., Kurauchi-Mito, A., Bokuda, K., Narita, T., Oshima, Y., Sakoda, M., Tamai, Y., Sato, H., Fukuda, K., and Itoh, H. (2010) The (pro)renin receptor/ATP6AP2 is essential for vacuolar H⁺-ATPase assembly in murine cardiomyocytes. *Circ. Res.* **107**, 30–34
 65. Oshima, Y., Kinouchi, K., Ichihara, A., Sakoda, M., Kurauchi-Mito, A., Bokuda, K., Narita, T., Kurosawa, H., Sun-Wada, G. H., Wada, Y., Yamada, T., Takemoto, M., Saleem, M. A., Quaggin, S. E., and Itoh, H. (2011) Prorenin receptor is essential for normal podocyte structure and function. *J. Am. Soc. Nephrol.* **22**, 2203–2212
 66. Davidson, H., Rhodes, C. J., Hutton, J. C. (1988) Intraorganellar calcium and pH control proinsulin cleavage in the pancreatic β -cell via two distinct site-specific endopeptidases. *Nature* **333**, 93–96
 67. Orci, L., Halban, P., Perrelet, A., Amherdt, M., Ravazzola, M., and Anderson, R. G. (1994) pH-independent and -dependent cleavage of proinsulin in the same secretory vesicle. *J. Cell Biol.* **126**, 1149–1156